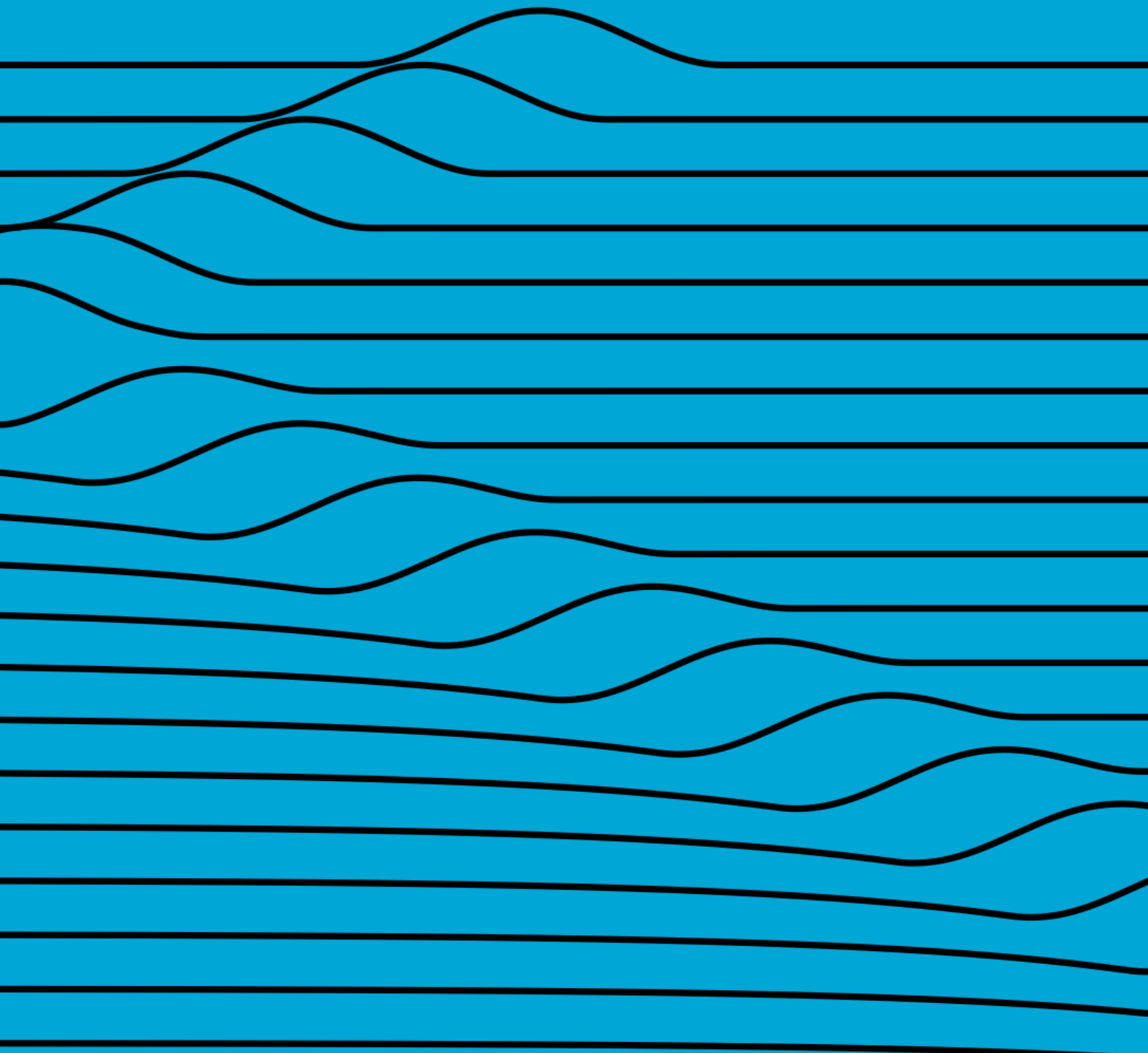


# Vibrations of a nonlinear string with a nonlinear quasi-zero stiffness system as a boundary condition

J. van de Velde



TU DELFT

APPLIED MATHEMATICS

THESIS REPORT

---

Vibrations of a nonlinear string with a  
nonlinear quasi-zero stiffness system as a  
boundary condition

---

*By:*  
JEROEN VAN DE VELDE  
4962354

*Supervisor/Thesis committee chair:*  
DR.IR. W.T. VAN HORSSSEN  
*Thesis committee member:*  
DR.IR. S. JAIN

May 16, 2025

# Contents

<b>Abstract</b>	<b>ii</b>
<b>1 Introduction</b>	<b>1</b>
<b>2 Derivation system of equations</b>	<b>2</b>
2.1 Nonlinear string equation . . . . .	2
2.2 Nonlinear boundary condition . . . . .	4
2.3 Nondimensionalization . . . . .	5
2.4 Other formulations . . . . .	6
2.4.1 Integral representation . . . . .	7
2.4.2 Series solution . . . . .	8
<b>3 Asymptotic expansion</b>	<b>9</b>
3.1 Extended oblique springs . . . . .	9
3.1.1 First order: d'Alembert solution . . . . .	9
3.1.2 Second order . . . . .	10
3.1.3 Energy analysis . . . . .	12
3.2 Compressed oblique springs . . . . .	14
<b>4 Multiple time scales</b>	<b>17</b>
4.1 Extended oblique springs . . . . .	17
4.1.1 First order: Laplace Transform . . . . .	17
4.1.2 Root finding characteristic function: $Q(s)$ . . . . .	19
4.1.3 First order solution . . . . .	21
4.1.4 Second order; second time scale . . . . .	22
4.2 Compressed oblique springs . . . . .	26
4.2.1 Unstable region . . . . .	26
4.2.2 Stable region . . . . .	31
4.2.3 Energy analysis . . . . .	34
<b>5 Conclusion</b>	<b>37</b>
<b>A Appendix: Code</b>	<b>39</b>

## Abstract

Vibrations in engineering structures can lead to severe instabilities, especially under low-frequency excitations that traditional linear isolators cannot effectively suppress. To address this, quasi-zero stiffness (QZS) vibration isolators, known for their high-static-low-dynamic stiffness properties, have gained increasing attention. This report investigates the reflection and absorption characteristics of a nonlinear string with a QZS mechanism applied as a boundary condition. The model is considered, and the governing equations are derived and nondimensionalized. Using regular perturbation methods and the method of multiple time scales, analytical solutions are obtained and evaluated. The analysis distinguishes between cases where the oblique springs are extended or compressed. It is found that with compressed springs, when the vertical damping coefficient is below unity, the system is counterintuitively stable. Furthermore, the inclusion of oblique dampers leads to unphysical energy growth. These phenomena are attributed to the singular nature of the system's dynamics and the limitations of the chosen multiple time scale method. The results indicate that the current model does not fully capture the effects of the oblique springs and dampers, underscoring the need for further investigation into the system's asymptotic expansions. Moreover, exploring second-order dynamics and external forcing could provide a deeper understanding of the system's complex behaviour.

# 1 Introduction

Vibrations in structures such as high-rise buildings and bridges pose significant engineering challenges. Under different kinds of forcing, these vibrations can be amplified, leading to instabilities or even catastrophic failure. One of the most famous example of this is the Tacoma Narrows bridge, which collapsed a few months after its opening due to the oscillations caused by strong winds. More recently, the Erasmusbrug in the Netherlands experienced severe rain-wind-induced vibrations in its cables, prompting the installation of hydraulic dampers to suppress those vibrations [1].

Traditionally, linear vibration isolation systems are used to mitigate such effects. However, linear isolators are only effective when the excitation frequency exceeds  $\sqrt{2}$  times the system's natural frequency [2]. This limits the effectiveness for excitations with low-frequency components [3]. To circumvent this problem, nonlinear/quasi-zero stiffness (QZS) vibration isolators have been proposed, and over the past two decades, research has increased significantly [4].

A QZS isolator uses a positive stiffness mechanism and a negative stiffness mechanism, which is generally nonlinear. This mechanism gives the system a high-static-low-dynamic stiffness (HSLDS), which enables the isolators to mitigate low-frequency vibration effectively while maintaining static load stability [4]. Among various QZS, designs one of the most studied is the three-spring configuration, originally proposed by Molyneux in 1957 [5]. It consists of two oblique compressed springs, which generate the negative stiffness characteristic, and one vertical spring.

Carrella et al. [6], [7] considered this system and focused on the static behaviour and transmissibility. Yan et al. [8] used the harmonic balance method to understand the bistable dynamics. The system is often approximated as a Duffing oscillator to analyse its nonlinear response, as such Brennan et al. [9] calculated the jump-up and jump-down frequencies of the Duffing oscillator. The model has also been extended by Qui et al. [10] to include a nonlinear damper, which saw increased performance. Recently, Xie et al. [11] investigated the effects of QZS systems on bridges, showing promising results in suppressing low modal frequencies.

Despite these advances, the wave reflection and absorption properties of QZS systems when used as boundary conditions have not been thoroughly investigated. This report addresses that gap

In [Section 2](#), the system of equations is derived. Here the nonlinear string equation and the boundary condition are obtained, and the system is nondimensionalized. An asymptotic expansion is performed, which is solved with the method of d'Alembert in [Section 3](#). In [Section 4](#), the model is expanded by introducing multiple time scales, which is solved using the Laplace transform. Finally, the findings are concluded in [Section 5](#) and recommendations are made for future research.

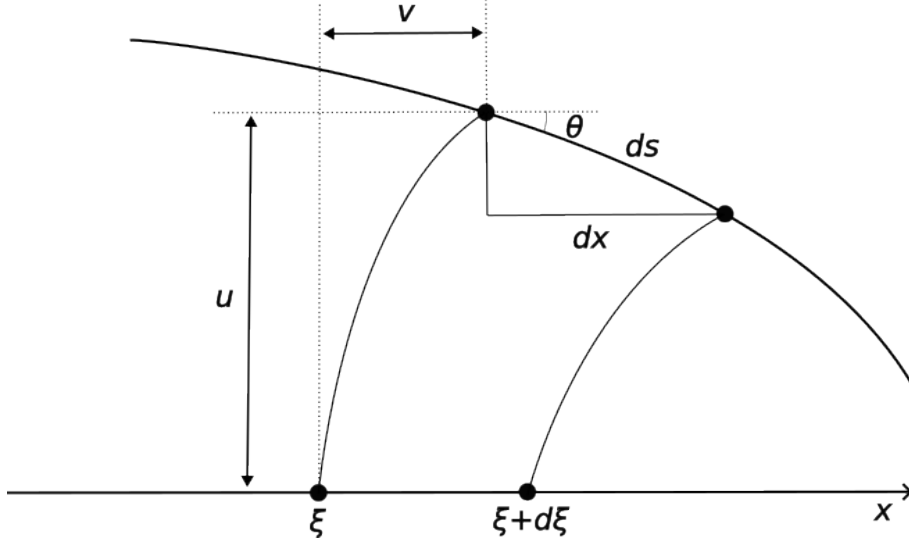


**Figure 1:** Diagram of the string and its stretched state with the relevant quantities displayed.

## 2 Derivation system of equations

### 2.1 Nonlinear string equation

For the derivation of the nonlinear string equation, we will follow the steps proposed by Narashima [12]. We consider a string stretched from 0 to  $L_*$ , where at  $x = L_*$  the string is fixed. At  $x = 0$ , we have the nonlinear vibration isolator. The nonlinear boundary condition will be derived in Section 2.2. We assume that there is no longitudinal displacement at  $x = 0$ . The longitudinal displacement is denoted by  $v = v(x, t)$  and the transverse displacement is denoted by  $u = u(x, t)$ .

We consider the string with the  $x$ -axis defined along the string at its equilibrium position, see Figure 1. The  $x$  coordinate is treated as a field coordinate, and to indicate a particular particle, we use its position  $\xi$  at rest as a label, so we have that  $\xi$  is the Lagrangian coordinate. The initial position  $\xi$  and the position  $x$  at time  $t$  are related by

$$\xi(x, t) = x - v(x, t). \quad (2.1)$$

Thus for the full time derivative we can see that

$$\frac{d}{dt} = \frac{\partial}{\partial t} + \frac{dx}{dt} \frac{\partial}{\partial x} = \frac{\partial}{\partial t} + \frac{dv}{dt}(x, t) \frac{\partial}{\partial x}. \quad (2.2)$$

If we now consider the element  $d\xi$  of the string, which is stretched to  $ds$  during motion, then we have by definition

$$\frac{ds}{d\xi} = \sqrt{1 + \left(\frac{\partial u}{\partial x}\right)^2}. \quad (2.3)$$

The tension forces in the  $v$  and  $u$  directions are given as

$$T_v = T \cos \theta = T \frac{dx}{ds}, \quad (2.4a)$$

$$T_u = T \sin \theta = T \frac{du}{ds}, \quad (2.4b)$$

where  $\theta$  is the angle of the string and the  $x$ -axis. By balancing the forces on the element  $ds$  we obtain

$$m \frac{d^2 v}{dt^2} = \frac{dx}{ds} \frac{\partial}{\partial x} \left( T \frac{dx}{ds} \right) + Q_v, \quad (2.5a)$$

$$m \frac{d^2 u}{dt^2} = \frac{dx}{ds} \frac{\partial}{\partial x} \left( T \frac{du}{ds} \right) + Q_u + R, \quad (2.5b)$$

where  $Q_v$  is the force working in the  $x$  direction,  $Q_u$  is the force working in the direction normal to  $x$ , and  $R$  represents whatever damping forces may be present. Finally,  $m = m(x, t)$  is the mass per unit length.

Due to the conservation of mass, we have that

$$m(x, t)ds = m_0(\xi)d\xi, \quad (2.6)$$

where  $m_0(\xi)$  is the value of  $m$  of the string at rest. By combining [Equations \(2.1\)](#) and [\(2.6\)](#) we can write

$$m \frac{ds}{dx} = m_0(\xi) \frac{d\xi}{dx} = \left(1 - \frac{dv}{dx}\right) m_0(x - v). \quad (2.7)$$

To complete the system of equations, we need to relate the tension  $T$  with the displacements. For this, we make the following assumptions

1. The string is very thin,
2. The material of the string is a linear elastic solid.

Assumption 1 gives that the stress can be taken to be nearly uniform. The second assumption gives that the tension at any point is the product of the Young's modulus  $E$ , the cross-sectional area  $A$  and the linear strain  $e$ . Thus the tension can be written as [\[12\]](#)

$$T = T_0(1 + c_1^2\lambda - c_2^2\lambda^2 + c_3^2\lambda^3), \quad (2.8)$$

where  $T_0$  is the initial tension at equilibrium,  $\lambda$  is the apparent strain given by

$$\lambda \equiv \frac{ds}{d\xi} - 1, \quad (2.9)$$

and the other constants are given by

$$c_1^2 = \frac{1}{\lambda_0} - 2\nu', \quad c_2^2 = \frac{2\nu'}{\lambda_0} - \nu'^2, \quad c_3^2 = \frac{\nu'^2}{\lambda_0}. \quad (2.10)$$

Here  $\lambda_0 = e_0/(1 + e_0)$  is the effective strain and  $\nu' = \nu(1 + e_0)/(1 - \nu e_0)$  is the effective Poisson's ratio, with  $e_0$  as the initial strain and  $\nu$  as Poisson's ratio.

Using [Equations \(2.1\)](#) and [\(2.3\)](#),  $\lambda$  can be expressed as

$$\lambda \equiv \frac{ds}{d\xi} - 1 = \frac{dx}{d\xi} \frac{ds}{dx} - 1 = \frac{\sqrt{1 + u_x^2}}{1 - v_x} - 1, \quad (2.11)$$

where the subscripts denote partial derivatives.

Now [Equation \(2.5\)](#) can be written as

$$(1 - v_x)\ddot{v} = \frac{T_0}{m_0} \frac{\partial}{\partial x} (\Lambda) + \tilde{Q}_v, \quad (2.12a)$$

$$(1 - v_x)\ddot{u} = \frac{T_0}{m_0} \frac{\partial}{\partial x} (u_x \Lambda) + \tilde{Q}_u + \tilde{R}, \quad (2.12b)$$

where  $\tilde{Q}_v = Q_v/m_0$  and similarly for  $\tilde{Q}_u$  and  $\tilde{R}$ . Furthermore, we have defined

$$\Lambda \equiv \frac{1 + c_1^2\lambda - c_2^2\lambda^2 + c_3^2\lambda^3}{(1 + \lambda)(1 - v_x)}. \quad (2.13)$$

We note that the strains in the string are usually small thus  $\lambda$  and  $\lambda_0$  are small and the  $c_i$  ( $i = 1, 2, 3$ ) are large. Thus we can expand [Equation \(2.11\)](#) into

$$\lambda = v_x + \frac{1}{2}u_x^2 + v_x^2 - \frac{1}{8}u_x^2(u_x^2 - 4v_x) + \dots \quad (2.14)$$

So we can also assume that the amplitudes of the oscillations are small. The most significant non-linear problem arises when  $v = \mathcal{O}(u^2)$ . If  $v$  is of a higher order, then from [Equation \(2.12a\)](#) we would have that in the first order  $\Lambda$  is independent of  $x$ , and so  $u_x$  is also independent of  $x$ . On the other hand, if  $v$  is of a

lower order, then Equation (2.12b) would reduce to a linear equation for  $u$  in the first order. Thus, we will assume that

$$v = \mathcal{O}(\varepsilon^2), \quad u = \mathcal{O}(\varepsilon), \quad \lambda = \mathcal{O}(\varepsilon^2), \quad (2.15)$$

where  $\varepsilon$  is a small parameter. Then we can expand  $\Lambda$  as follows

$$\Lambda = 1 + c_1^2 \lambda + c_2^2 \lambda^2 + (v_x - \lambda)(1 + c_1^2 \lambda) + \mathcal{O}(\varepsilon^4). \quad (2.16)$$

Putting this into Equation (2.12b) and comparing orders of magnitude, we see that the left-hand side is of  $\mathcal{O}(\varepsilon)$  and the right-hand side is of  $\mathcal{O}(\varepsilon) + \mathcal{O}(c_1^2 \varepsilon^3)$ .  $c_1^2$  is large so there is no a priori justification for ignoring the second term on the right-hand side unless  $\varepsilon$  is extremely small. Furthermore, if we take  $\varepsilon$  to be extremely small we would obtain the linear string equation. Thus we consider the following limiting process

$$\varepsilon \rightarrow 0, \quad c_1^2 \rightarrow \infty, \quad c_1^2 \varepsilon^2 \equiv \Gamma = \mathcal{O}(1), \quad (2.17)$$

where  $\Gamma$  is held fixed. Since  $c_2^2$  and  $c_3^2$  are of the same order of magnitude as  $c_1^2$  we can also say that  $c_2^2 \varepsilon^2 = c_3^2 \varepsilon^2 = \mathcal{O}(1)$ . Additionally, we assume that there is no longitudinal forcing so  $\tilde{Q}_v \equiv 0$ . For the transverse forcing, we assume that  $\tilde{Q}_u = \mathcal{O}(\varepsilon)$ , since for the amplitude to be small the forcing also needs to be small.

Now using that  $v = \varepsilon^2 \hat{v}$ ,  $u = \varepsilon \hat{u}$  and  $\tilde{Q}_u = \varepsilon \hat{Q}_u$  we see that

$$\varepsilon^2 v_{tt} = \frac{T_0}{m_0} \Gamma \frac{\partial}{\partial x} \left( v_x + \frac{1}{2} u_x^2 \right) + \mathcal{O}(\varepsilon^2) \quad (2.18a)$$

$$u_{tt} = \frac{T_0}{m_0} u_{xx} + \frac{T_0}{m_0} \Gamma \frac{\partial}{\partial x} \left[ u_x \left( v_x + \frac{1}{2} u_x^2 \right) \right] + \tilde{R} + Q_u + \mathcal{O}(\varepsilon^2), \quad (2.18b)$$

where we have dropped the  $\hat{\cdot}$  for brevity.

If we neglect the left-hand side in Equation (2.18a) we can see that

$$v_x + \frac{1}{2} u_x^2 = A(t). \quad (2.19)$$

The function  $A(t)$  can be found by integrating the above to obtain

$$A(t) = \frac{1}{L_*} \left[ v(L_*, t) - v(0, t) + \frac{1}{2} \int_0^{L_*} u_x^2 dx \right] = \frac{1}{2L_*} \int_0^{L_*} u_x^2 dx, \quad (2.20)$$

where we used that  $v(L_*, t) = v(0, t) = 0$ , since at  $x = L_*$  the string is fixed and that at  $x = 0$  we assumed no longitudinal displacement. Finally, we obtain the equation

$$u_{tt} = \frac{T_0}{m_0} \left( 1 + \frac{\Gamma}{2L_*} \int_0^{L_*} u_x^2 dx \right) u_{xx} + \tilde{R} + Q_u. \quad (2.21)$$

## 2.2 Nonlinear boundary condition

In Figure 2, the configuration of the springs and dampers is shown. We have two oblique springs with stiffness  $\kappa_*$  and two oblique linear dampers with damping coefficient  $\alpha_*$ . Furthermore, we have a vertical linear damper with coefficient  $\beta_*$ . If  $u(0, t) = 0$  then we denote the length of the spring as  $\ell_*$  and the equilibrium length of the spring is  $\ell_{0*}$ . The angle  $\phi$  is the angle of the spring with the horizontal. We have assumed that there is no longitudinal motion, so  $v(0, t) = 0$ .

We have chosen for a two spring system, without the vertical springs, to reduce the number of components and ease the mathematical derivation. Furthermore, without the vertical spring, we can focus on the investigation of the contributions of the oblique springs.

We have four forces working on the string: the force of the springs  $F_s$ , of the oblique damper  $F_{o-d}$ , of the vertical damper  $F_{v-d}$  and of the string tension  $F_T$ . We have assumed that there is no horizontal movement at the boundary so we only need to consider the force balance in the vertical direction.

First, we consider  $F_{T,v}$ , where the subscript  $v$  denotes the vertical component. We have that

$$F_{T,v} = T_0 \sin \theta = T_0 \frac{u_x}{\sqrt{1 + u_x^2}}. \quad (2.22)$$

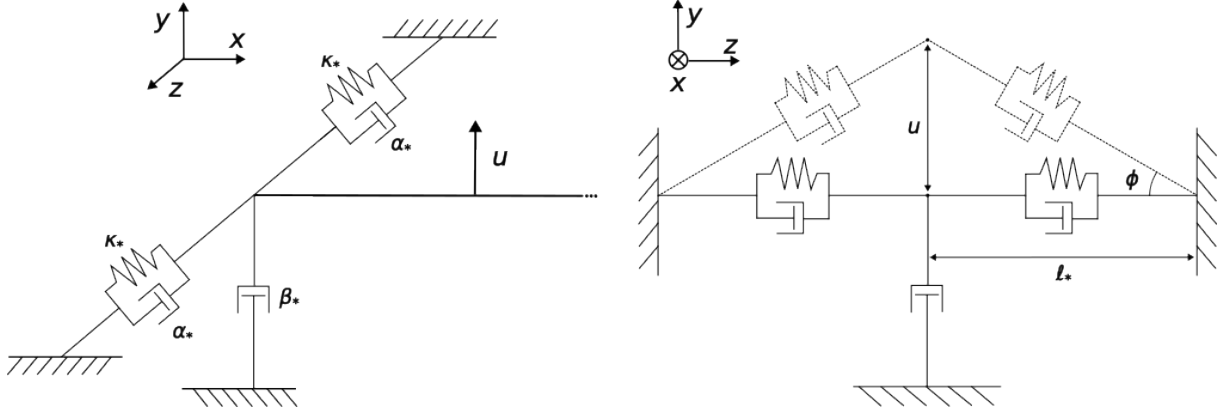


**Figure 2:** Diagram of the nonlinear system at the boundary  $x = 0$ . The left diagram is of a 3-dimensional view of the system with the string, and the right diagram is a head-on view of the system.

Here  $\theta$  is the angle of the string and  $u_x = u_x(0, t)$ , where, for the sake of brevity, the evaluation is not included in the following formulas.

The force of the spring and the damper is dependent on the length  $w = \sqrt{u^2 + \ell_*^2}$ . So we have that

$$F_{s,v} = -2 \sin(\phi) \kappa_* (w - \ell_{0*}) = -2u\kappa_* \left(1 - \frac{\ell_{0*}}{w}\right), \quad (2.23)$$

$$= -2u\kappa_* \left(1 - \frac{\ell_{0*}}{\sqrt{u^2 + \ell_*^2}}\right). \quad (2.24)$$

For the oblique damper force, we need to calculate

$$\frac{d}{dt} \sqrt{u^2 + \ell_*^2} = \frac{uu_t}{\sqrt{u^2 + \ell_*^2}}. \quad (2.25)$$

Now we can see that

$$F_{o-d,v} = -2\alpha_* \sin(\phi) \frac{d}{dt} \sqrt{u^2 + \ell_*^2} = -2\alpha_* \frac{u^2 u_t}{u^2 + \ell_*^2}. \quad (2.26)$$

The force of the vertical damper is given as

$$F_{v-d} = -\beta_* u_t. \quad (2.27)$$

Thus by balancing the forces we can see that

$$T_0 \frac{u_x}{\sqrt{1 + u_x^2}} = 2u\kappa_* \left(1 - \frac{\ell_{0*}}{\sqrt{u^2 + \ell_*^2}}\right) + \beta_* u_t + 2\alpha_* \frac{u^2}{u^2 + \ell_*^2} u_t. \quad (2.28)$$

### 2.3 Nondimensionalization

We have obtained the following system of equations

$$u_{tt}(x, t) = \frac{T_0}{m_0} \left(1 + \frac{\Gamma}{2L_*} \int_0^{L_*} u_x^2(\xi, t) d\xi\right) u_{xx}(x, t) + R(x, t) + Q_u(x, t), \quad 0 < x < L_*, t > 0, \quad (2.29a)$$

$$T_0 \frac{u_x}{\sqrt{1 + \varepsilon^2 u_x^2}} = 2u\kappa_* \left(1 - \frac{\ell_{0*}}{\sqrt{\varepsilon^2 u^2 + \ell_*^2}}\right) + \beta_* u_t + 2\alpha_* \frac{\varepsilon^2 u^2}{\varepsilon^2 u^2 + \ell_*^2} u_t, \quad x = 0, t > 0, \quad (2.29b)$$

$$u(L, t) = 0, \quad t > 0, \quad (2.29c)$$

$$u(x, 0) = f(x), \quad 0 < x < L_*, \quad (2.29d)$$

$$u_t(x, 0) = g(x), \quad 0 < x < L_*, \quad (2.29e)$$

where the  $\varepsilon$  is added in Equation (2.29b) since in the derivation of Equation (2.29a) the assumption  $u = \varepsilon \hat{u}$  was made. To non-dimensionalize this system we introduce the following non-dimensional coordinates and quantities

$$u^*(x^*, t^*) = \frac{u(x, t)}{L^*}, \quad x^* = \frac{x}{L^*}, \quad t^* = \frac{t}{T^*}, \quad f^*(x^*) = \frac{f(x)}{L^*}, \quad g^*(x^*) = g(x) \frac{T^*}{L^*}, \quad (2.30)$$

$$R^*(x^*, t^*) = R(x, t) \frac{(T^*)^2}{L^*}, \quad Q^*(x^*, t^*) = Q_u(x, t) \frac{(T^*)^2}{L^*}, \quad (2.31)$$

where  $L^*$  and  $T^*$  are the characteristic length and time, respectively, chosen such that  $T_0/m_0 = (L^*/T^*)^2$ . Substituting this into Equation (2.29b) we obtain the following, where we have omitted the  $(0, t^*)$ ,

$$\frac{u_{x^*}^*}{\sqrt{1 + \varepsilon^2 (u_{x^*}^*)^2}} = 2u \frac{\kappa_* L^*}{T_0} \left( 1 - \frac{\ell_{0^*}/L^*}{\sqrt{\varepsilon^2 (u^*)^2 + (\ell_*/L^*)^2}} \right) + \frac{\beta_* L^*}{T_0 T^*} u_{t^*}^* + 2 \frac{\alpha_* L^*}{T_0 T^*} \frac{\varepsilon^2 (u^*)^2}{\varepsilon^2 (u^*)^2 + (\ell_*/L^*)^2} u_{t^*}^*. \quad (2.32)$$

To reduce the number of parameters in the equation, we choose  $L^* = \ell_*$  and we introduce the non-dimensional constants

$$\ell_0 = \frac{\ell_{0^*}}{\ell_*}, \quad L = \frac{L^*}{\ell_*}, \quad \kappa = \frac{\kappa_* \ell_*}{T_0}, \quad \beta = \frac{\beta_* \ell_*}{T_0 T^*} = \frac{\beta_*}{\sqrt{m_0 T_0}}, \quad \alpha = \frac{\alpha_* \ell_*}{T_0 T^*} = \frac{\alpha_*}{\sqrt{m_0 T_0}}. \quad (2.33)$$

So if the oblique springs are compressed in the horizontal position, then  $\ell_0 > 1$ . Lastly, we assume that  $L \gg 1$ , such that  $\delta = \ell_*/L \ll 1$  is a small parameter. Thus now we have obtained the non-dimensional system, where we have dropped the superscript  $*$ ,

$$u_{tt}(x, t) = \left( 1 + \delta \frac{\Gamma}{2} \int_0^L u_x^2(\xi, t) d\xi \right) u_{xx}(x, t) + R(x, t) + Q(x, t), \quad 0 < x < L, t > 0, \quad (2.34a)$$

$$\frac{u_x}{\sqrt{1 + \varepsilon^2 u_x^2}} = 2u\kappa \left( 1 - \frac{\ell_0}{\sqrt{1 + \varepsilon^2 u^2}} \right) + \beta u_t + 2\alpha \frac{\varepsilon^2 u^2}{1 + \varepsilon^2 u^2} u_t, \quad x = 0, t > 0, \quad (2.34b)$$

$$u(L, t) = 0, \quad t > 0, \quad (2.34c)$$

$$u(x, 0) = f(x), \quad 0 < x < L, \quad (2.34d)$$

$$u_t(x, 0) = g(x), \quad 0 < x < L. \quad (2.34e)$$

The equations for the left boundary condition are highly nonlinear. So as an approximation, we will use the first terms of the Taylor series [10], [13]. We have that

$$F_{T,v} \approx \left[ u_x - \frac{1}{2} \varepsilon^2 u_x^3 + \frac{3}{8} \varepsilon^4 u_x^5 \right], \quad (2.35)$$

$$F_{s,v} \approx -\kappa \left[ 2(1 - \ell_0)u + \ell_0 \varepsilon^2 u^3 - \frac{3\ell_0}{4} \varepsilon^4 u^5 \right], \quad (2.36)$$

$$F_{d,v} \approx -2\alpha u_t [\varepsilon^2 u^2 - \varepsilon^4 u^4]. \quad (2.37)$$

Taking only up to the cubic terms we see that the force balance becomes

$$u_x(0, t) - \frac{1}{2} \varepsilon^2 u_x^3(0, t) = \lambda u(0, t) + \kappa \ell_0 \varepsilon^2 u^3(0, t) + \beta u_t(0, t) + 2\alpha \varepsilon^2 u^2(0, t) u_t(0, t), \quad (2.38)$$

where we have defined  $\lambda = 2\kappa(1 - \ell_0)$ .

## 2.4 Other formulations

In the derivation of Equation (2.21) we made various assumptions. In the following, we present two different approaches which aim to lessen the assumptions placed on the problem. By doing so, a greater portion of the system's full dynamics is retained, offering a clearer view of the effects and interactions that are omitted in the final equation. Although these expressions proved too complex to be included in the subsequent analysis, they provide valuable insights and reveal opportunities for deeper exploration in future work.

### 2.4.1 Integral representation

To obtain Equation (2.21), we neglected the left-hand side of Equation (2.18a). However, this transforms the hyperbolic equation into a parabolic equation. Furthermore, since we had to integrate over the domain to obtain  $A(t)$ , we had to assume that the string was finite. To consider an infinite string, we can keep the left-hand side of the equation and consider the higher orders of the right-hand side as perturbations of the hyperbolic part. So then we can solve the following system for  $v$

$$\begin{aligned} v_{tt} &= c^2 [v_{xx} + u_x u_{xx}], & x > 0, t > 0, \\ v(0, t) &= 0, & t > 0, \\ v(x, 0) &= f_v(x), \quad v_t(x, 0) = g_v(x), & x > 0. \end{aligned}$$

Here  $c^2 = T_0 \Gamma / (m_0 \varepsilon^2)$  and  $f_v(x)$  and  $g_v(x)$  are the initial position and velocity respectively. We assume that there is no energy at  $\infty$ , so  $v$  and all its derivatives are zero for  $x \rightarrow \infty$ .

Now we have a linear wave equation in  $v$  with the forcing  $F(x, t) = c^2 u_x u_{xx}$ . We know that the solution is given by

$$v(x, t) = \frac{1}{2} [f_v(x + ct) + f_v(x - ct)] + \frac{1}{2c} \int_{x-ct}^{x+ct} g_v(\xi) d\xi + \frac{1}{2c} \int_0^t \int_{x-c(t-\tau)}^{x+c(t-\tau)} F(\xi, \tau) d\xi d\tau. \quad (2.39)$$

If  $x - ct > 0$ , then we can evaluate the first integral of the last term to obtain

$$\begin{aligned} v(x, t) &= \frac{1}{2} [f_v(x + ct) + f_v(x - ct)] + \frac{1}{2c} \int_{x-ct}^{x+ct} g_v(\xi) d\xi \\ &\quad + \frac{c}{4} \int_0^t [u_x^2(x + c(t - \tau), \tau) - u_x^2(x - c(t - \tau), \tau)] d\tau. \end{aligned} \quad (2.40)$$

For the substitution, we need to know  $v_x$ . So we obtain the following, where the notation  $p = x + c(t - \tau)$  and  $m = x - c(t - \tau)$  was used to keep the formula concise,

$$\begin{aligned} v_x(x, t) &= \frac{1}{2} [f'_v(x + ct) + f'_v(x - ct)] + \frac{1}{2c} [g_v(x + ct) - g_v(x - ct)] \\ &\quad + \frac{c}{2} \int_0^t [u_x(p, \tau) u_{xx}(p, \tau) d\tau - u_x(m, \tau) u_{xx}(m, \tau)] d\tau. \end{aligned} \quad (2.41)$$

The functions  $f_v$ ,  $g_v$  and  $u$  are only defined for  $x > 0$ , so we need to adjust the formula if  $x - ct < 0$ . Since we have the left boundary condition  $v(0, t) = 0$ , we take the odd extensions of  $f_v$ ,  $g_v$  and  $F$ . To determine the forcing term, we first define  $t_0 = t - x/c$ . The time  $t_0$  is the time it takes for the wave from point  $x$  to reach the boundary. So for times  $\tau < t_0$  we need to consider the influence of the boundary. We have that

$$\begin{aligned} \int_0^t \int_{x-c(t-\tau)}^{x+c(t-\tau)} F(\xi, \tau) d\xi d\tau &= \int_{t_0}^t \int_{x-c(t-\tau)}^{x+c(t-\tau)} F(\xi, \tau) d\xi d\tau + \int_0^{t_0} \int_0^{x+c(t-\tau)} F(\xi, \tau) d\xi d\tau \\ &\quad + \int_0^{t_0} \int_{x-c(t-\tau)}^0 F(\xi, \tau) d\xi d\tau. \end{aligned} \quad (2.42)$$

Above, we can see that we only need to consider the odd extension for the last term. Thus, if  $x - ct < 0$ , then we have that

$$\begin{aligned} v(x, t) &= \frac{1}{2} [f_v(x + ct) - f_v(ct - x)] + \frac{1}{2c} \int_{ct-x}^{x+ct} g_v(\xi) d\xi \\ &\quad + \frac{c}{4} \left\{ \int_0^t u_x^2(x + c(t - \tau), \tau) d\tau - \int_{t_0}^t u_x^2(x - c(t - \tau), \tau) d\tau - \int_0^{t_0} u_x^2(c(t - \tau) - x, \tau) d\tau \right\}. \end{aligned} \quad (2.43)$$

Furthermore, the derivative  $v_x$ , is given as

$$\begin{aligned} v_x(x, t) &= \frac{1}{2} [f'_v(x + ct) + f'_v(ct - x)] + \frac{1}{2c} [g_v(x + ct) + g_v(ct - x)] \\ &\quad + \frac{c}{2} \left\{ \int_0^t u_x(p, \tau) u_{xx}(p, \tau) d\tau - \int_{t_0}^t u_x(m, \tau) u_{xx}(m, \tau) d\tau + \int_0^{t_0} u_x(-m, \tau) u_{xx}(-m, \tau) d\tau \right\}. \end{aligned} \quad (2.44)$$

### 2.4.2 Series solution

To solve the nonlinear equation [Equation \(2.21\)](#), one can represent  $u$  as a Fourier series or apply the Laplace transform. We will try to obtain a series solution for the whole system of [Equation \(2.18\)](#). The series we use is

$$v(x, t) = \sum_{n \geq 1} V_n(t) \sin\left(\frac{n\pi}{L}x\right), \quad (2.45)$$

$$u(x, t) = \sum_{n \geq 0} U_n(t) \phi_n(x), \quad (2.46)$$

where  $\phi_n(x)$  is the solution of the system

$$\phi_n''(x) + \mu_n^2 \phi_n(x) = 0, \quad 0 < x < L, \quad (2.47)$$

$$\phi_n'(0) = \lambda \phi_n(0), \quad (2.48)$$

$$\phi_n(L) = 0. \quad (2.49)$$

This system was obtained by considering the linear first-order part of [Equations \(2.18\)](#) and [\(2.34\)](#) and using separation of variables. Furthermore, we assumed  $\beta = 0$ , since complications arise for  $\beta > 0$  and we want to focus on the interaction between the equations in this section.

So we have that

$$\phi_n(x) = \sin(\mu_n x) + \frac{\mu_n}{\lambda} \cos(\mu_n x) \quad (2.50)$$

with  $\mu_n$  given by the solutions of

$$\sin(\mu_n L) + \frac{\mu_n}{\lambda} \cos(\mu_n L) = 0. \quad (2.51)$$

We can see that  $\mu_0 = 0$  and  $\mu_n \approx (n + 1/2)\pi/L$  as  $n$  becomes large. Furthermore, one can show that

$$\int_0^L \phi_n \phi_m dx = 0, \quad \text{for } n \neq m. \quad (2.52)$$

Now substituting these series into [Equation \(2.18\)](#) and using the orthogonality of  $\sin(n\pi x/L)$  and  $\phi_n$  for [Equations \(2.18a\)](#) and [\(2.18b\)](#) respectively, we obtain

$$\varepsilon^2 \dot{V}_n = -\Gamma \left(\frac{n\pi}{L}\right)^2 V_n - \frac{2\Gamma}{L} \int_0^L u_x u_{xx} \sin\left(\frac{n\pi x}{L}\right) dx, \quad (2.53a)$$

$$\ddot{U}_n = -\mu_n^2 U_n - \frac{\Gamma}{\Phi_n} \int_0^L \left\{ v_x u_{xx} + u_x v_{xx} + \frac{3}{2} u_x^2 u_{xx} \right\} \phi_n(x) dx, \quad (2.53b)$$

where  $\Phi_n = \int_0^L \phi_n^2 dx$ . Now we need to evaluate the integrals to see how the modes interact with each other. We will consider the cubic term as an example. Then we have

$$\int_0^L u_x^2 u_{xx} \phi_n(x) dx = \sum_i \sum_j \sum_k U_i U_j U_k \int_0^L \phi_i' \phi_j' \phi_k'' \phi_n dx \quad (2.54)$$

$$= \sum_i \sum_j \sum_k -U_i U_j U_k \mu_k^3 \mu_j (\mu_i^2 + \mu_j^2 - \mu_k^2 - \mu_n^2) \mu_i \mu_n A_{ijkn}, \quad (2.55)$$

with  $A_{ijkn}$  a fraction composed of  $\mu_i, \mu_j, \mu_k$  and  $\mu_n$ . We can see that only the modes with one of the  $\mu_i, \mu_j, \mu_k$  or  $\mu_n$  equal to zero and  $(\mu_i^2 + \mu_j^2 - \mu_k^2 - \mu_n^2) = 0$  do not have an interaction with this term. Furthermore, since there is no closed expression of  $\mu_n$  it is difficult to evaluate the indices for which this happens. So there are an infinite number of interactions between the two equations.

### 3 Asymptotic expansion

To solve the system of Equation (2.34), we will use an asymptotic expansion. However, in the system we have two small parameters:  $\delta$  and  $\varepsilon$ . Since we have  $\delta = \ell_*/L$ , we can choose  $L$  to obtain different orders of  $\delta$  concerning  $\varepsilon$ . We consider the case  $\delta = \mathcal{O}(\varepsilon^2)$ .

We perform the asymptotic expansion on  $\delta = \varepsilon^2$ , so we have that

$$u(x, t) = u_0(x, t) + \varepsilon^2 u_1(x, t) + \mathcal{O}(\varepsilon^4). \quad (3.1)$$

Now we substitute the above expression into Equation (2.34) with the boundary condition as Equation (2.38). Then we collect the terms of different orders of  $\varepsilon$ .

#### 3.1 Extended oblique springs

In the asymptotic analysis, we separate the two cases where the oblique springs are extended or compressed. These cases have respectively  $\ell_0 \leq 1$  and  $\ell_0 > 1$ . For the extended case, we have that  $\lambda \geq 0$ , and for the compressed case, we have that  $\lambda < 0$ .

We have to consider the compressed case separately since the first order force is only the outward component. In the second order, a restoring force becomes present, however, this means that two diverging functions have to balance.

##### 3.1.1 First order: d'Alembert solution

The system we obtain for the first order is

$$\mathcal{O}(1) : u_{0,tt}(x, t) = u_{0,xx}(x, t), \quad 0 < x < L, t > 0, \quad (3.2a)$$

$$u_{0,x}(0, t) = \lambda u_0(0, t) + \beta u_{0,t}(0, t), \quad t > 0, \quad (3.2b)$$

$$u_0(L, t) = 0, \quad t > 0, \quad (3.2c)$$

$$u_0(x, 0) = f(x), \quad u_{0,t}(x, 0) = g(x), \quad 0 < x < L, \quad (3.2d)$$

with  $\lambda = 2\kappa(1 - \ell_0)$ . We can see that we need to solve the wave equation with non-standard boundary conditions. This system has been studied in [14] and we will follow a similar procedure.

The solution of the wave equation is given by the d'Alembert solution, which is given as

$$u_0(x, t) = \frac{1}{2}f(x+t) + \frac{1}{2}f(x-t) + \frac{1}{2} \int_{x-t}^{x+t} g(s) ds. \quad (3.3)$$

However, for  $x-t < 0$  the functions  $f$  and  $g$  are not defined. So we need to use the boundary condition to define these. We consider the following equation

$$u_0(x, t) = \frac{1}{2}f(x+t) + \frac{1}{2} \int_0^{x+t} g(s) ds + \frac{1}{2}\varphi(t-x). \quad (3.4)$$

and we substitute it in Equation (3.2b). We then obtain the differential equation

$$\varphi'(t) + \kappa_0 \varphi(t) = - \left( \kappa_0 \left[ f(t) + \int_0^t g(s) ds \right] + \gamma_0 [f'(t) + g(t)] \right) \equiv -h(t), \quad (3.5)$$

with

$$\kappa_0 = \frac{\lambda}{1 + \beta} = \frac{2\kappa(1 - \ell_0)}{1 + \beta}, \quad \gamma_0 = \frac{\beta - 1}{\beta + 1}. \quad (3.6)$$

The solution of the differential equation is given as

$$\varphi(t) = f(0)e^{-\kappa_0 t} - e^{-\kappa_0 t} \int_0^t e^{\kappa_0 s} h(s) ds, \quad (3.7)$$

where we used that  $u(0, 0) = f(0)$  gives  $\varphi(0) = f(0)$ . Now replacing  $t$  by  $t-x$  and performing integration by parts where possible for  $h(s)$ , we obtain from Equation (3.4), for  $x-t < 0$ ,

$$\begin{aligned} u_0(x, t) &= \frac{1}{2}f(x+t) - \frac{1}{2}\gamma_0 f(t-x) + \frac{1}{2}(\gamma_0 + 1)f(0)e^{\kappa_0(x-t)} + \frac{1}{2} \int_{t-x}^{x+t} g(s) ds \\ &\quad + \frac{1}{2}\kappa_0(\gamma_0 - 1)e^{\kappa_0(x-t)} \int_0^{t-x} e^{\kappa_0 s} f(s) ds - \frac{1}{2}(\gamma_0 - 1)e^{\kappa_0(x-t)} \int_0^{t-x} e^{\kappa_0 s} g(s) ds. \end{aligned} \quad (3.8)$$

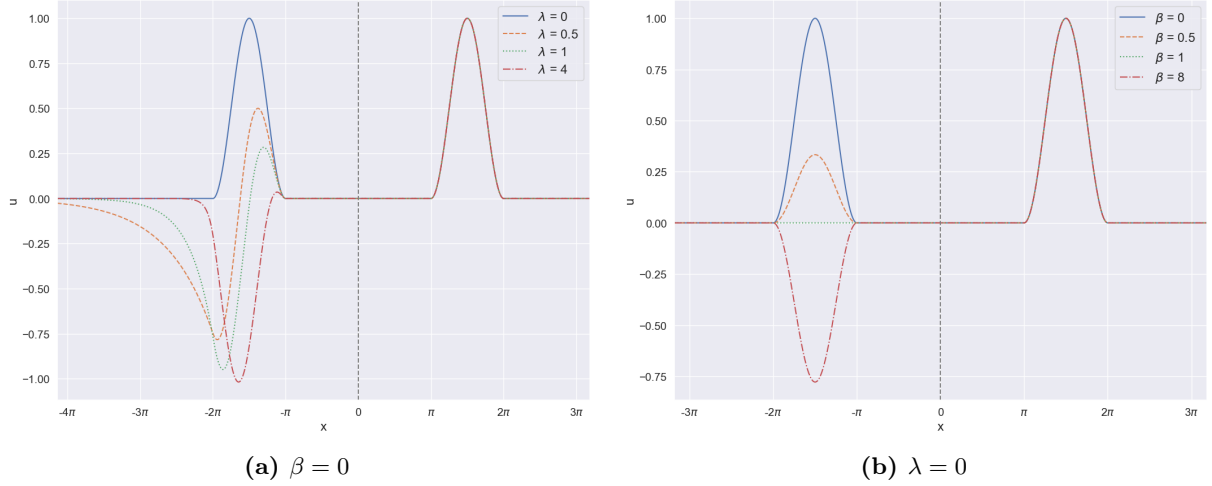


**Figure 3:** Reflections of the first order solutions for different values of  $\lambda$  and  $\beta$ .

We consider an initial wave which travels to the left, so we have that  $g(x) = f'(x)$ . Then we can see that for  $x - t > 0$  we obtain

$$u_0(x, t) = f(x + t). \quad (3.9)$$

For  $x - t < 0$  we have that

$$u_0(x, t) = f(x + t) - \gamma_0 f(t - x) + \gamma_0 f(0) e^{\kappa_0(x-t)} + \kappa_0(\gamma_0 - 1) e^{\kappa_0(x-t)} \int_0^{t-x} e^{\kappa_0 s} f(s) ds. \quad (3.10)$$

In [Figure 3](#) we have shown the reflection,  $x < 0$ , of the wave with initial conditions  $f(x) = \sin^2(x)$  and  $g(x) = f'(x)$  on  $\pi \leq x \leq 2\pi$  and  $f(x) = 0$  elsewhere. The reflections are shown for different values of  $\lambda$  and  $\beta$ . We can see that we have an even extension in the case of  $\beta = \lambda = 0$  and an odd extension in the limiting cases  $\beta = 0, \lambda \rightarrow \infty$  and  $\lambda = 0, \beta \rightarrow \infty$ .

### 3.1.2 Second order

The system we obtain for the second order is

$$\mathcal{O}(\varepsilon^2) : u_{1,tt}(x, t) = u_{1,xx}(x, t) + F(x, t), \quad 0 < x < L, t > 0, \quad (3.11a)$$

$$u_{1,x}(0, t) = \lambda u_1(0, t) + \beta u_{1,t}(0, t) + G(t), \quad t > 0, \quad (3.11b)$$

$$u_1(L, t) = 0, \quad t > 0, \quad (3.11c)$$

$$u_1(x, 0) = u_{1,t}(x, 0) = 0, \quad 0 < x < L, \quad (3.11d)$$

where the forcing terms in the wave equation and boundary condition are given as

$$F(x, t) = \frac{\Gamma}{2} u_{0,xx}(x, t) \int_0^L u_{0,x}^2(\xi, t) d\xi, \quad (3.12)$$

$$G(t) = \kappa \ell_0 u_0^3(0, t) + 2\alpha u_0^2(0, t) u_{0,t}(0, t) + \frac{1}{2} u_{0,x}^3(0, t). \quad (3.13)$$

[Equation \(3.11a\)](#) is the wave equation with forcing, for which the solution is known as

$$u_1(x, t) = \frac{1}{2} \int_0^t \int_{x-(t-\tau)}^{x+t-\tau} F(\xi, \tau) d\xi d\tau. \quad (3.14)$$

If  $x - t > 0$ , then we can see that  $\xi - \tau > 0$  holds for the whole integration domain. Thus,  $u_1(x, t)$  is fully defined. However, if  $x - t < 0$ , then the integral in [Equation \(3.14\)](#) needs to be split into four parts, which are shown in [Figure 4](#). In the region I, we have that  $\xi - \tau > 0$  and in the regions II and III we have  $\xi - \tau < 0$ . In region IV  $F(\xi, \tau)$  is not defined since it is a function of  $u_0$  and it is not defined for  $x < 0$ .

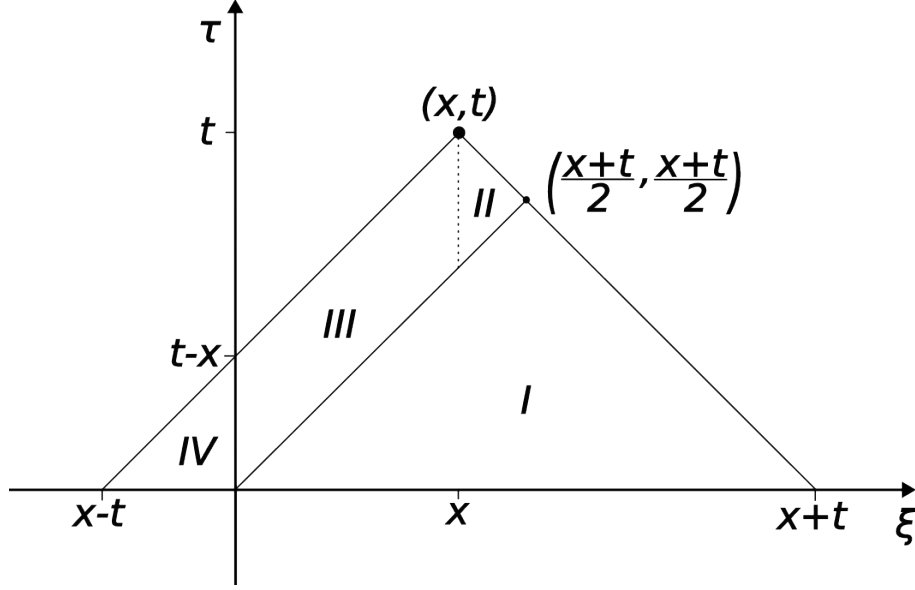


Figure 4: Diagram of the cone of integration for Equation (3.14)

As in the first order, we will use the boundary condition to define this part of the function. Thus, we have that

$$u_1(x, t) = \frac{1}{2} \int_0^{(x+t)/2} \int_{\tau}^{x+t-\tau} F(\xi, \tau) d\xi d\tau + \frac{1}{2} \int_x^{(x+t)/2} \int_{\xi}^{x+t-\xi} F(\xi, \tau) d\tau d\xi \quad (3.15)$$

$$+ \frac{1}{2} \int_0^x \int_{\xi}^{t-(x-\xi)} F(\xi, \tau) d\tau d\xi + \frac{1}{2} \varphi(t-x),$$

where the function  $\varphi$  has to be determined. We substitute this into Equation (3.11b) and we obtain the following differential equation

$$\varphi'(t) + \kappa_0 \varphi(t) = -\gamma_0 \int_0^{t/2} F(t-\tau, \tau) d\tau - \gamma_0 \int_{t/2}^t F(t-\tau, \tau) d\tau - \kappa_0 \left[ \int_0^{t/2} \int_{\tau}^{t-\tau} F(\xi, \tau) d\xi d\tau \right. \quad (3.16)$$

$$\left. + \int_0^{t/2} \int_{\xi}^{t-\xi} F(\xi, \tau) d\tau d\xi \right] - \frac{2}{1+\beta} G(t)$$

$$\equiv -H(t), \quad (3.17)$$

where  $\kappa_0$  and  $\gamma_0$  are defined as in Equation (3.6). Thus we have that

$$\varphi(t) = C_1 e^{-\kappa_0 t} - e^{-\kappa_0 t} \int_0^t e^{\kappa_0 s} H(s) ds. \quad (3.18)$$

Since  $u_1(x, 0) = 0$ , we can see that  $u_1(0, 0) = 0$ . Thus, as an initial condition, we have  $\varphi(0) = u_1(0, 0) = 0$ . So, it follows that  $C_1 = 0$ .

Now by again replacing  $t$  with  $t-x$  we see that

$$u_1(x, t) = \frac{1}{2} \int_0^{(x+t)/2} \int_{\tau}^{x+t-\tau} F(\xi, \tau) d\xi d\tau + \frac{1}{2} \int_x^{(x+t)/2} \int_{\xi}^{x+t-\xi} F(\xi, \tau) d\tau d\xi \quad (3.19)$$

$$+ \frac{1}{2} \int_0^x \int_{\xi}^{t-(x-\xi)} F(\xi, \tau) d\tau d\xi - \frac{1}{2} e^{\kappa_0(x-t)} \int_0^{t-x} e^{\kappa_0 s} H(s) ds,$$

with

$$H(t) = \gamma_0 \int_0^{t/2} F(t-\tau, \tau) d\tau + \gamma_0 \int_{t/2}^t F(t-\tau, \tau) d\tau + \kappa_0 \int_0^{t/2} \int_{\tau}^{t-\tau} F(\xi, \tau) d\xi d\tau \quad (3.20)$$

$$+ \kappa_0 \int_0^{t/2} \int_{\xi}^{t-\xi} F(\xi, \tau) d\tau d\xi + \frac{2}{1+\beta} G(t).$$

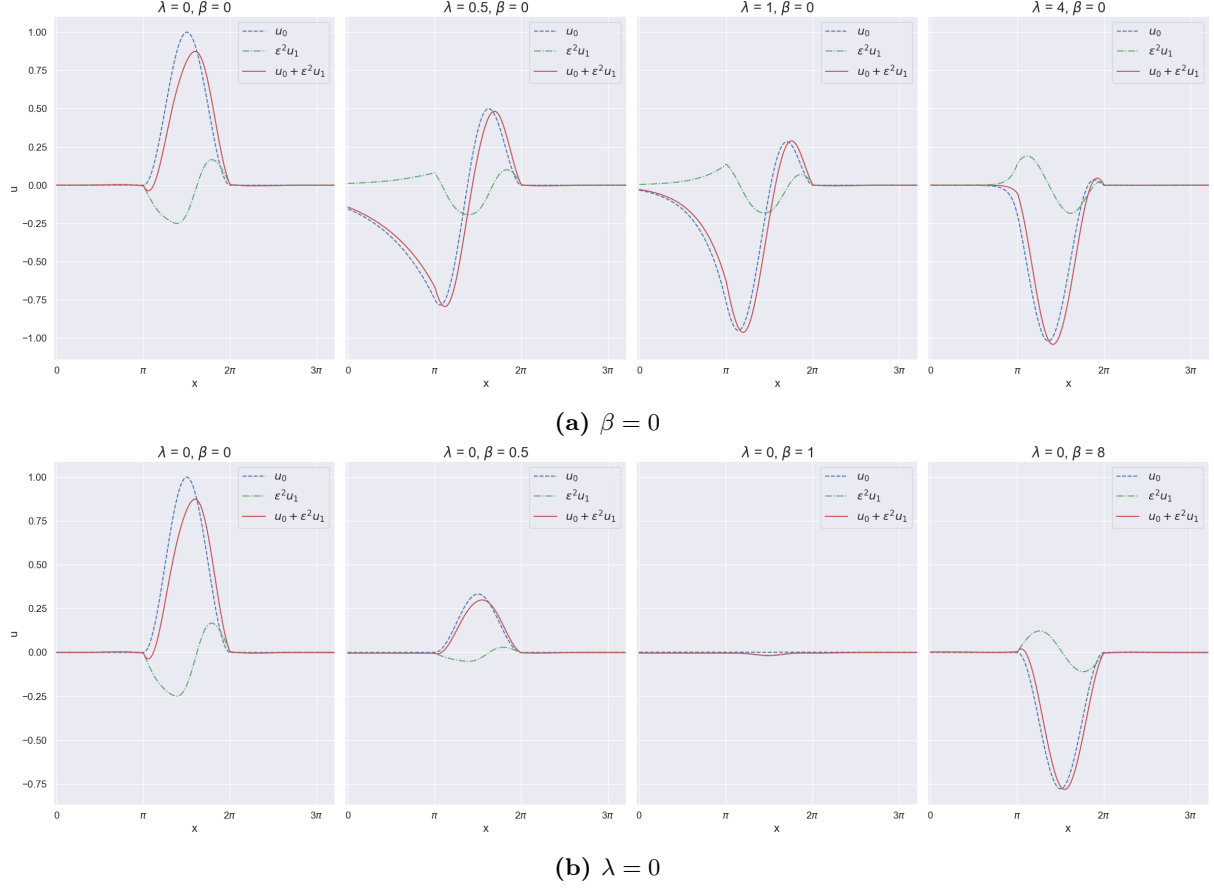


**Figure 5:** Reflections for extended springs plotted at  $t = 3\pi$  for different values of  $\lambda$  and  $\beta$ .

In [Figure 5](#), the first-order and the second-order reflections are shown for multiple values of  $\lambda$  and  $\beta$  at time  $t = 3\pi$ . In the simulations we used  $\ell_0 = 1/2$ ,  $\alpha = 1$ ,  $\Gamma = 1$  and  $L = 30$ . For the remainder of this report, we will use the values  $\Gamma = 1$  and  $L = 30$ . In the plots, we can see that the second-order term has a significant contribution. Furthermore, in [Figure 6](#), we have plotted the case of  $\beta = \lambda = 0$  for different values of  $t$ . Here we can see that the second order contribution grows over time.

### 3.1.3 Energy analysis

To further investigate the effect and growth of the second-order term, we can calculate the energy of the system. To determine the energy, we multiply [Equation \(2.34a\)](#) with  $u_t$  and we integrate with respect to  $x$  from 0 to  $L$ . So then we obtain

$$0 = \int_0^L u_{tt} u_t dx - \left( 1 + \varepsilon^2 \frac{\Gamma}{2} \int_0^L u_x^2 dx \right) \int_0^L u_{xx} u_t dx \quad (3.21)$$

$$= \frac{d}{dt} \int_0^L \frac{1}{2} u_t^2 dx - \left( 1 + \varepsilon^2 \frac{\Gamma}{2} \int_0^L u_x^2 dx \right) \left( [u_x u_t]_0^L - \int_0^L u_x u_{xt} dx \right) \quad (3.22)$$

$$= \frac{d}{dt} \int_0^L \frac{1}{2} [u_t^2 + u_x^2] dx + \frac{d}{dt} \varepsilon^2 \frac{\Gamma}{4} \left( \int_0^L u_x^2 dx \right)^2 + \left( 1 + \varepsilon^2 \frac{\Gamma}{2} \int_0^L u_x^2 dx \right) u_x(0, t) u_t(0, t). \quad (3.23)$$

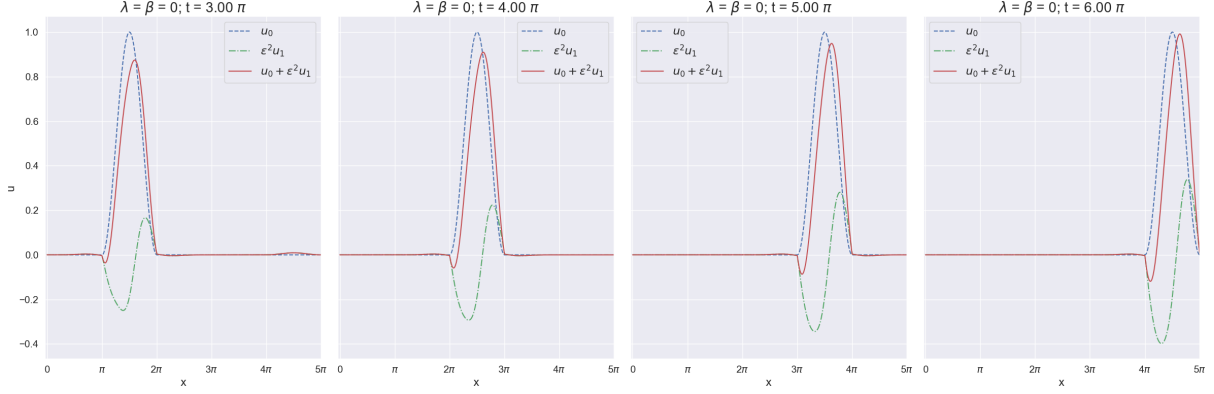


**Figure 6:** Reflections for extended springs with  $\lambda = \beta = 0$  plotted for different times.

Now with [Equation \(2.34b\)](#) we have that

$$u_x(0, t)u_t(0, t) = \sqrt{1 + \varepsilon^2 u_x^2(0, t)} \left[ 2u(0, t)u_t(0, t)\kappa \left( 1 - \frac{\ell_0}{\sqrt{1 + \varepsilon^2 u^2(0, t)}} \right) + u_t^2(0, t) \left( \beta + 2\alpha \frac{\varepsilon^2 u^2(0, t)}{1 + \varepsilon^2 u^2(0, t)} \right) \right] \quad (3.24)$$

$$= \sqrt{1 + \varepsilon^2 u_x^2(0, t)} \left[ \frac{d}{dt} \frac{\kappa}{\varepsilon^2} (\sqrt{1 + \varepsilon^2 u^2(0, t)} - \ell_0)^2 + u_t^2(0, t) \left[ \beta + 2\alpha \frac{\varepsilon^2 u^2(0, t)}{1 + \varepsilon^2 u^2(0, t)} \right] \right]. \quad (3.25)$$

Now if we denote

$$V(t) = \left( 1 + \varepsilon^2 \frac{\Gamma}{2} \int_0^L u_x^2 dx \right) \sqrt{1 + \varepsilon^2 u_x^2(0, t)} - 1 \quad (3.26)$$

then we have that

$$\begin{aligned} \frac{d}{dt} \int_0^L \frac{\varepsilon^2}{2} [u_t^2 + u_x^2] dx + \frac{d}{dt} \varepsilon^4 \frac{\Gamma}{4} \left( \int_0^L u_x^2 dx \right)^2 + (1 + V(t)) \frac{d}{dt} \kappa \left[ \sqrt{1 + \varepsilon^2 u^2(0, t)} - \ell_0 \right]^2 \\ = -(1 + V(t)) u_t^2(0, t) \left[ \beta + 2\alpha \frac{\varepsilon^2 u^2(0, t)}{1 + \varepsilon^2 u^2(0, t)} \right] \end{aligned} \quad (3.27)$$

In the left-hand side of the above equation, we first have the derivative of the linear energy of the string and then we have the derivative of the energy contributed by the nonlinear term. Lastly, we have on the left-hand side the derivative of the energy stored in the springs multiplied by a correction term,  $1 + V(t)$ . This correction term appears because we assumed for the boundary condition that  $v(0, t) = 0$ , so we could not do the same reduction concerning  $v$  as for the string equation. However, we can see that  $V(t) = \mathcal{O}(\varepsilon^2)$  and that the derivative of the spring energy is of order  $\mathcal{O}(\varepsilon^2)$ , so this correction only matters in the orders of  $\varepsilon^4$  or above.

Since  $1 + V(t) \geq 0$ , we can see that the right-hand side of [Equation \(3.27\)](#) is less than or equal to zero. So we have that

$$\frac{d}{dt} E(t) + \mathcal{O}(\varepsilon^4) \leq 0, \quad (3.28)$$

where we have defined the energy  $E(t)$  as

$$E(t) = \int_0^L \frac{\varepsilon^2}{2} [u_t^2 + u_x^2] dx + \kappa (\sqrt{1 + \varepsilon^2 u^2(0, t)} - \ell_0)^2. \quad (3.29)$$

Thus, we see that the energy of the system cannot increase over time.

In [Figure 7](#), the energy is plotted, where the left plot shows the energy of  $u_0$  and the right plot shows the energy of  $u_0 + \varepsilon^2 u_1$ . In both plots, the energy is shifted such that it is zero at  $t = 0$ . The plots are

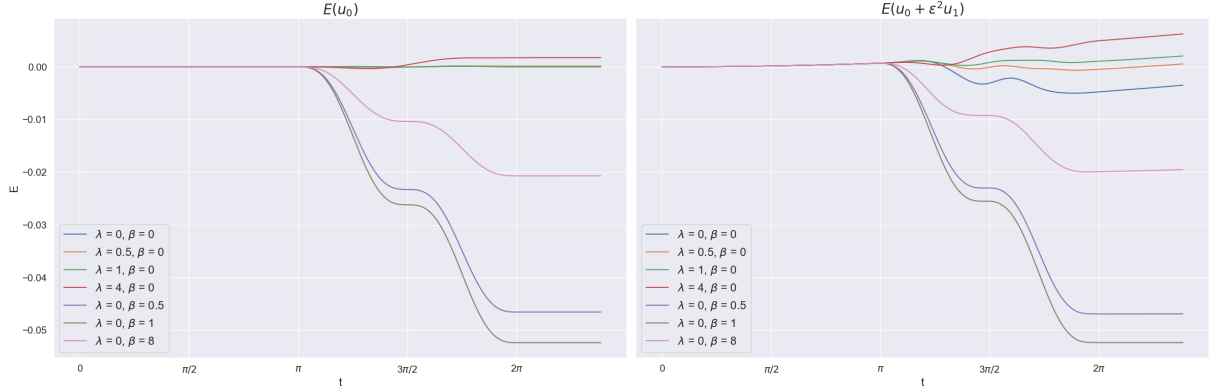


**Figure 7:** Energy of  $u_0$  and  $u_0 + \varepsilon^2 u_1$  for different values of  $\lambda$  and  $\beta$ .

shifted instead of normalised to better show the increase in energy for the second-order terms. Since then, the increase would be less visible for higher values of  $\lambda$  because the higher values of  $\kappa$  lead to a higher total energy.

In the first plot, we can see that in most cases with  $\beta = 0$  the energy in the system stays constant. For  $\lambda = 4$ , there is a small increase in the energy during the boundary interaction, however, this is due to computation errors in the numerical integration and the way the plots are presented. Due to computation errors, the string does not completely settle back at  $u = 0$  after the boundary interaction and a higher  $\lambda$  increases that error more. The way the plots are presented leads to the error being visible, since if the energies were normalised, the increase in error due to  $\lambda$  would be balanced by the increase in total energy.

For different values of  $\beta$ , we have different amounts of damping. In the case of  $\beta = 1$ , we have perfect damping, so there is no energy left in the system. As  $\beta \rightarrow \infty$ , we can see that there is less damping since the system approaches a fixed-end boundary.

But if we now consider the second plot, we can see that in all cases the energy increases with time, and this violates the conservation of energy of the system. This is because the asymptotic analysis introduces secular terms as forcing for the second-order problem. These secular terms grow over time and cause this increase in energy. The increase in energy is not yet visible after the boundary for the cases  $\beta = 1$  and  $\beta = 1/2$ , however, this is because the system is heavily damped. Since the growth of the second order is relative to the first order, it is not yet visible.

### 3.2 Compressed oblique springs

In the case of compressed springs, the above solution is not valid, since the solution blows up. This is what we expect in the first order, since we only have the outward force of the springs. Consequently, the second order also diverges, and the balancing of those two diverging solutions does not result in a valid solution. Furthermore, we will see that the stable equilibrium solution is at order  $\mathcal{O}(1/\varepsilon)$ , and so to reach that solution, we would violate our ordering assumptions. We solve this by making an extra assumption on  $\lambda$ . Namely, we assume that  $|\lambda| = \mathcal{O}(\varepsilon^2)$ . This way, the system is out of the compression region after a small perturbation.

There are multiple ways to obtain the order assumption on  $\lambda$ . We will assume that

$$\ell_0 = 1 + \rho\varepsilon^2. \quad (3.30)$$

Then we have that  $\lambda = -2\rho\kappa\varepsilon^2 = -\hat{\lambda}\varepsilon^2$ . Another way is to use the three spring system and tune the spring coefficients such that the linear force only has a small contribution [6].

We can use the solutions of the extended spring case with some adaptations. The outward force of the oblique springs is shifted to the second order. Thus, for the first order, we have the same system as Equation (3.2) but with  $\lambda = 0$ . Accordingly we have Equation (3.8) as a solution but with  $\kappa_0 = 0$ . Hence we have that

$$u_0(x, t) = \frac{1}{2}f(x+t) - \frac{1}{2}\gamma_0 f(t-x) + \frac{1}{2}(\gamma_0 + 1)f(0) + \frac{1}{2} \int_{t-x}^{x+t} g(s) ds - \frac{1}{2}(\gamma_0 - 1) \int_0^{t-x} g(s) ds. \quad (3.31)$$

Similarly, for the second order, we have the system Equation (3.11) with  $\lambda = 0$ . Additionally, we need

to change the forcing in the boundary condition to

$$G_{compr}(t) = -\hat{\lambda}u_0(0,t) + \kappa\ell_0u_0^3(0,t) + \alpha u_0^2(0,t)u_{0,t}(0,t) + \frac{1}{2}u_{0,x}^3(0,t). \quad (3.32)$$

The second order solution is then

$$u_1(x,t) = \frac{1}{2} \iint_{I,II,III} F(\xi,\tau) d\xi d\tau - \frac{1}{2} \int_0^{t-x} H_{compr}(s) ds, \quad (3.33)$$

with

$$H_{compr}(t) = \gamma_0 \int_0^{t/2} F(t-\tau,\tau) d\tau + \gamma_0 \int_{t/2}^t F(t-\tau,\tau) d\tau + \frac{2}{1+\beta} G_{compr}(t). \quad (3.34)$$

Since we consider the case of compressed springs, it is important to know what the eventual equilibrium positions of the system are. The equilibrium solutions,  $u_{eq}$ , can be found by setting  $u_{eq,t} = 0$  and then solving the system of Equation (2.34). From Equations (2.34a) and (2.34c) we see that  $u_{eq} = m(1-x/L)$ , where  $m$  needs to be determined from the other boundary condition, eq. (2.34b). So we need to solve for  $m$  in

$$\frac{-\frac{m}{L}}{\sqrt{1+\varepsilon^2 m^2/L^2}} = 2m\kappa \left(1 - \frac{\ell_0}{\sqrt{1+\varepsilon^2 m^2}}\right). \quad (3.35)$$

This has no clear analytical solution, except for  $m = 0$ , which corresponds with the unstable equilibrium point. However, since  $L = 1/\varepsilon^2$  we can see that the left-hand side of the equation is equal to  $-\frac{m}{L}$  up to order  $\mathcal{O}(\varepsilon^6)$ . Then we need to solve for

$$-\frac{\varepsilon^2}{2\kappa} = 1 - \frac{\ell_0}{\sqrt{1+\varepsilon^2 m^2}}. \quad (3.36)$$

It follows that

$$m^2 = \frac{1}{\varepsilon^2} \left( \frac{\ell_0^2}{(1+\frac{\varepsilon^2}{2\kappa})^2} - 1 \right) = \frac{1}{\varepsilon^2} (\ell_{eq}^2 - 1), \quad (3.37)$$

corresponding to the stable equilibrium points. Above we have defined  $\ell_{eq} = \ell_0/(1+(2\kappa L)^{-1})$ , which is the length of the oblique springs at the stable equilibrium points. We can see that the equilibrium length is smaller than the rest length, where we have that if  $\kappa$  increases, then  $\ell_{eq}$  approaches  $\ell_0$ . So the stable equilibria are given by

$$u_{eq,st} = \pm m \left(1 - \frac{x}{L}\right) = \pm \frac{1}{\varepsilon} \sqrt{\frac{\ell_0^2}{(1+\frac{\varepsilon^2}{2\kappa})^2} - 1} \left(1 - \frac{x}{L}\right). \quad (3.38)$$

Here we can see that the stable equilibria are at a distance of order  $\mathcal{O}(1/\varepsilon)$ .

In Figure 8 we have plotted the reflections in the case of compressed springs with one of the stable equilibrium positions. Here we have chosen  $t = 3\pi$ ,  $\ell_0 = 1 + \varepsilon^2$ ,  $\Gamma = 1$ ,  $\beta = 1/2$  and  $\kappa \in [0, 1, 2, 4]$ , thus we have that  $\hat{\lambda} \in [0, 1, 2, 4]$ . We can see that as  $\kappa$  is increased, the stable equilibrium point of the system becomes more negative. However, only in the case of  $\kappa = 0$ , the boundary is at the equilibrium position. In the other cases, it is either slightly above the equilibrium position or significantly below the equilibrium position.

This due to the assumption that  $|\lambda| = \mathcal{O}(\varepsilon^2)$ . When we now want to calculate the equilibrium positions of each of the orders we see that we have

$$u_{0-eg,x}(0,t) = 0. \quad (3.39)$$

as boundary condition for  $x = 0$ . So we obtain that  $u_{0-eg} = 0$ . Following that, the second order boundary condition becomes  $u_{1-eg,x}(0,t) = 0$  and thus we also have that  $u_{1-eg} = 0$ . We can see this behaviour in Figure 8, where after the wave is away from the boundary and thus there is no change with respect to time, we have that the spatial derivative at the boundary is zero. The string at the boundary stays stuck at a position which is determined by the asymmetry created by the dampers and springs. For lower  $\kappa$ , this asymmetry is less strong, so the position at the boundary is closer to zero. Since the wave has no information yet about the right boundary, it will stay at this level. However, as the wave travels between the boundaries, it will eventually settle at zero due to damping at the boundary.

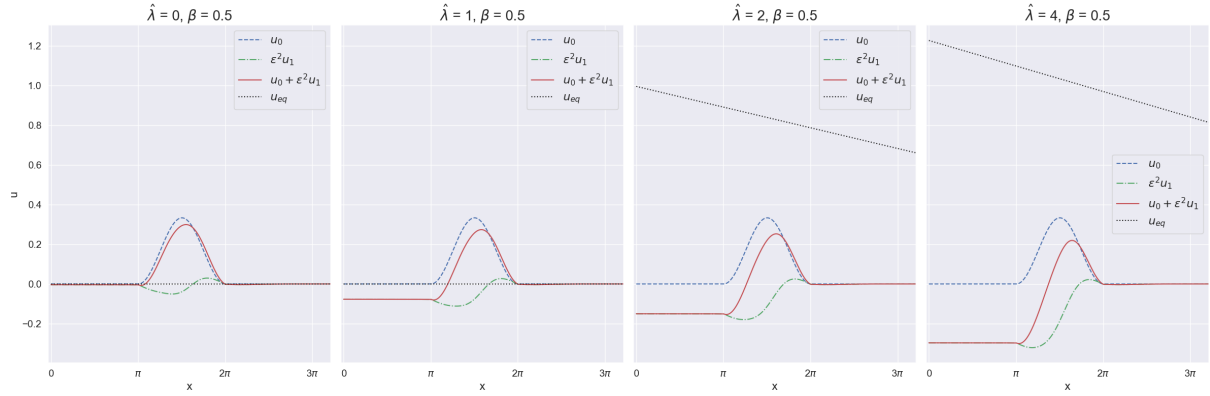


**Figure 8:** Reflections in the case of compressed springs with one of the stable equilibrium positions. The parameters chosen are  $t = 3\pi$ ,  $\ell_0 = 1 + \varepsilon^2$ ,  $\Gamma = 1$ ,  $\beta = 1/2$  and  $\kappa \in [0, 1, 2, 4]$ .

## 4 Multiple time scales

To remove the growth of the second-order term and to solve the problem of the equilibrium position with the compressed spring, we use the multiple time scale method. As our multiple time scales, we introduce the times  $t_0$  and  $t_1$  as

$$t_0 = t, \quad (4.1)$$

$$t_1 = \varepsilon^2 t. \quad (4.2)$$

So then we have that  $u = u(x, t_0, t_1)$  and the derivative with respect to  $t$  is transformed into

$$\frac{d}{dt} \rightarrow \frac{\partial}{\partial t_0} + \varepsilon^2 \frac{\partial}{\partial t_1}. \quad (4.3)$$

Now the system in Equation (2.34) with the boundary condition as Equation (2.38) becomes

$$u_{t_0 t_0} + 2\varepsilon^2 u_{t_0 t_1} + \varepsilon^4 u_{t_1 t_1} = \left(1 + \varepsilon^2 \frac{\Gamma}{2} \int_0^L u_x^2 d\xi\right) u_{xx}, \quad 0 < x < L, \quad t_0, t_1 > 0, \quad (4.4a)$$

$$u_x - \frac{1}{2}\varepsilon^2 u_x^3 = \lambda u + \kappa \ell_0 \varepsilon^2 u^3 + (\beta + 2\alpha \varepsilon^2 u^2) (u_{t_0} + \varepsilon^2 u_{t_1}), \quad x = 0, \quad t_0, t_1 > 0, \quad (4.4b)$$

$$u(L, t_0, t_1) = 0, \quad t_0, t_1 > 0, \quad (4.4c)$$

$$u(x, 0, 0) = f(x), \quad 0 < x < L, \quad (4.4d)$$

$$u_{t_0}(x, 0, 0) + \varepsilon^2 u_{t_1}(x, 0, 0) = g(x), \quad 0 < x < L. \quad (4.4e)$$

Now we again perform the asymptotic expansion on  $\varepsilon^2$ . We thus substitute the following expression into the above system

$$u(x, t_0, t_1) = u_0(x, t_0, t_1) + \varepsilon^2 u_1(x, t_0, t_1) + \mathcal{O}(\varepsilon^4). \quad (4.5)$$

If we collect orders, we obtain the first-order system as

$$u_{0,t_0 t_0} = u_{0,xx}, \quad 0 < x < L, \quad t_0, t_1 > 0, \quad (4.6a)$$

$$u_{0,x} = \lambda u_0 + \beta u_{0,t_0}, \quad x = 0, \quad t_0, t_1 > 0, \quad (4.6b)$$

$$u_0(L, t_0, t_1) = 0, \quad t_0, t_1 > 0, \quad (4.6c)$$

$$u_0(x, 0, 0) = f(x), \quad 0 < x < L, \quad (4.6d)$$

$$u_{0,t_0}(x, 0, 0) = g(x), \quad 0 < x < L. \quad (4.6e)$$

The second-order system is then given as

$$u_{1,t_0 t_0} = u_{1,xx} - 2u_{0,t_0 t_1} + \frac{\Gamma}{2} u_{0,xx} \int_0^L u_{0,x}^2 d\xi, \quad 0 < x < L, \quad t_0, t_1 > 0, \quad (4.7a)$$

$$u_{1,x} = \lambda u_1 + \beta u_{1,t_0} + \frac{1}{2} u_{0,x}^3 + \kappa \ell_0 u_0^3 + \beta u_{0,t_1} + 2\alpha u_0^2 u_{0,t_0}, \quad x = 0, \quad t_0, t_1 > 0, \quad (4.7b)$$

$$u_1(L, t_0, t_1) = 0, \quad t_0, t_1 > 0, \quad (4.7c)$$

$$u_1(x, 0, 0) = 0, \quad 0 < x < L, \quad (4.7d)$$

$$u_{1,t_0}(x, 0, 0) = -u_{0,t_1}(x, 0, 0), \quad 0 < x < L. \quad (4.7e)$$

In solving these equations, we again need to consider the cases of the extended and compressed springs separately. First, we start with the extended case.

### 4.1 Extended oblique springs

#### 4.1.1 First order: Laplace Transform

To solve the first-order system of equations (and the second-order), we use the Laplace transform. The Laplace transform is defined as

$$\mathcal{L}\{f\}(s) = \int_0^\infty f(t) e^{-st} dt = F(s), \quad (4.8)$$

where  $s$  is a complex number. Using the Laplace transform we can change the partial differential equation to an ODE, using the properties

$$\mathcal{L}\{f'\}(s) = sF(s) - f(0), \quad (4.9)$$

$$\mathcal{L}\{f''\}(s) = s^2F(s) - sf(0) - f'(0). \quad (4.10)$$

We apply the Laplace transform on the system eq. (4.6) with respect to  $t_0$ , so we have the transformation  $u_0(x, t_0, t_1) \rightarrow U_0(x, s, t_1)$ . For the  $t_0$  derivatives, we have

$$\mathcal{L}\{u_{x,t_0t_0}(x, t_0, t_1)\}(x, s, t_1) = s^2U_0(x, s, t_1) - su_0(x, 0, t_1) - u_{0,t_0}(x, 0, t_1) \quad (4.11)$$

$$= s^2U_0(x, s, t_1) - sa_0(x, t_1) - b_0(x, t_1), \quad (4.12)$$

$$\mathcal{L}\{u_{0,t_0}(0, t_0, t_1)\}(x, s, t_1) = sU_0(0, s, t_1) - a_0(x, t_1), \quad (4.13)$$

where  $a_0(x, t_1)$  and  $b_0(x, t_1)$  are functions we need to determine using the freedom added by the extra time scale. The functions need to satisfy the initial conditions

$$a_0(x, 0) = u_0(x, 0, 0) = f(x), \quad b_0(x, 0) = u_{0,t_0}(x, 0, 0) = g(x). \quad (4.14)$$

Now putting it together we obtain the system

$$U_{0,xx}(x, s, t_1) = s^2U_0(x, s, t_1) - sa_0(x, t_1) - b_0(x, t_1), \quad 0 < x < L, s \in \mathbb{C}, t_1 > 0, \quad (4.15a)$$

$$U_{0,x}(0, s, t_1) = (\lambda + \beta s)U_0(0, s, t_1) - \beta a_0(0, t_1), \quad s \in \mathbb{C}, t_1 > 0, \quad (4.15b)$$

$$U_0(L, s, t_1) = 0, \quad s \in \mathbb{C}, t_1 > 0. \quad (4.15c)$$

The solution of the differential equation is given as

$$U_0(x, s, t_1) = c_1(s, t_1)e^{sx} + c_2(s, t_1)e^{-sx} + \frac{e^{-sx}}{2s} \int_0^x h_0(\xi, s, t_1)e^{\xi s} d\xi - \frac{e^{sx}}{2s} \int_0^x h_0(\xi, s, t_1)e^{-\xi s} d\xi, \quad (4.16)$$

where  $h_0(x, s, t_1) = sa_0(x, t_1) + b_0(x, t_1)$ . The coefficients,  $c_1$  and  $c_2$ , are obtained from the boundary conditions, which give the following system of equations

$$(\kappa_0 + \gamma_0 s)c_1 + (\kappa_0 + s)c_2 = \frac{\beta}{\beta + 1}a_0(0, t_1), \quad (4.17)$$

$$c_1e^{sL} + c_2e^{-sL} = -\frac{e^{-sL}}{2s} \int_0^L h_0(\xi, s, t_1)e^{\xi s} d\xi + \frac{e^{sL}}{2s} \int_0^L h_0(\xi, s, t_1)e^{-\xi s} d\xi, \quad (4.18)$$

where the constants  $\kappa_0$  and  $\gamma_0$  are the same as defined in Equation (3.6). Solving the system, we obtain

$$c_1 = \frac{1}{Q(s)} \left[ (\kappa_0 + s)e^{2sL} \int_0^L h_0(\xi, s, t_1)e^{-\xi s} d\xi - (\kappa_0 + s) \int_0^L h_0(\xi, s, t_1)e^{\xi s} d\xi - 2s \frac{\beta}{\beta + 1} a_0(0, t_1) \right], \quad (4.19)$$

$$c_2 = \frac{1}{Q(s)} \left[ -(\kappa_0 + \gamma_0 s)e^{2sL} \int_0^L h_0(\xi, s, t_1)e^{-\xi s} d\xi + (\kappa_0 + \gamma_0 s) \int_0^L h_0(\xi, s, t_1)e^{\xi s} d\xi + 2se^{2sL} \frac{\beta}{\beta + 1} a_0(0, t_1) \right]. \quad (4.20)$$

$$Q(s) = 2s[(\kappa_0 + s)e^{2sL} - \gamma_0 s - \kappa_0]. \quad (4.21)$$

Finally, we have that

$$U_0(x, s, t_1) = \frac{P_0(x, s, t_1)}{Q(s)}, \quad (4.22)$$

$$\begin{aligned} P_0(x, s, t_1) = & \left[ -(\kappa_0 + \gamma_0 s) \int_0^L h_0(\xi, s, t_1)e^{-\xi s} d\xi + (\kappa_0 + s) \int_0^x h_0(\xi, s, t_1)e^{\xi s} d\xi + \frac{2s\beta}{\beta + 1} a_0(0, t_1) \right] e^{s(2L-x)} \\ & + (\kappa_0 + \gamma_0 s)e^{sx} \int_0^x h_0(\xi, s, t_1)e^{-\xi s} d\xi + (\kappa_0 + s)e^{s(2L+x)} \int_x^L h_0(\xi, s, t_1)e^{-\xi s} d\xi + \\ & (\kappa_0 + \gamma_0 s)e^{-sx} \int_x^L h_0(\xi, s, t_1)e^{\xi s} d\xi - \left[ (\kappa_0 + s) \int_0^L h_0(\xi, s, t_1)e^{\xi s} d\xi + \frac{2s\beta}{\beta + 1} a_0(0, t_1) \right] e^{sx}. \end{aligned} \quad (4.23)$$

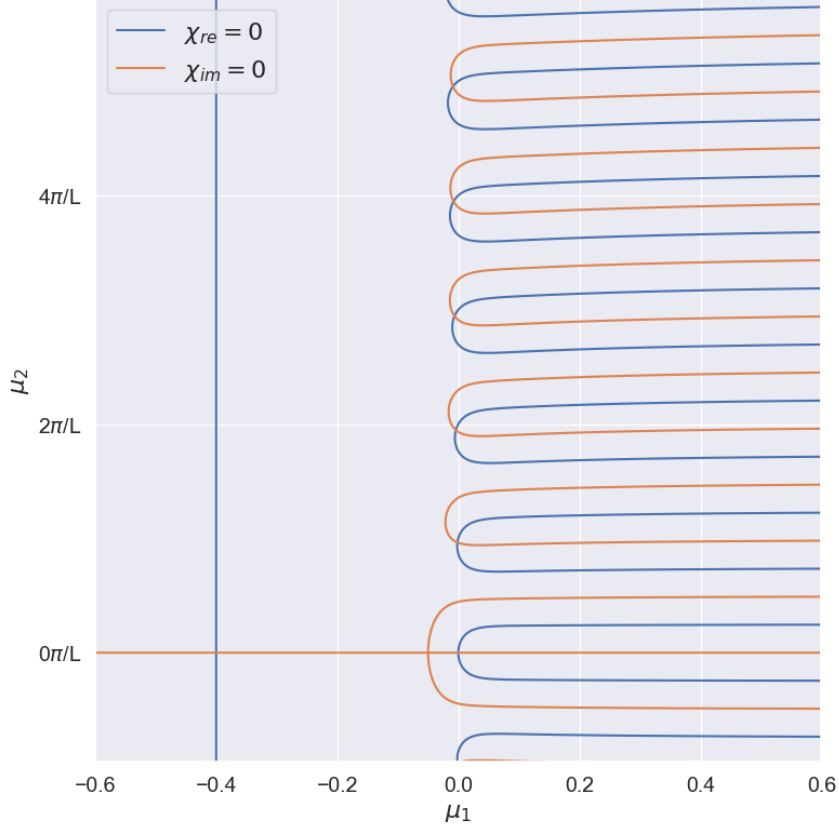


**Figure 9:** Contour lines of  $\chi_{re}(\mu_1, \mu_2) = 0$  and  $\chi_{im}(\mu_1, \mu_2) = 0$  for  $\kappa_0 = 1/5$  and  $\gamma_0 = 1/2$ .

To obtain  $u_0$  we need to use the inverse Laplace transform which is given as

$$f(t) = \mathcal{L}^{-1}\{F\}(t) = \frac{1}{2\pi i} \int_{\gamma-i\infty}^{\gamma+i\infty} F(s)e^{st} ds, \quad (4.24)$$

where  $\gamma$  is chosen such that all the poles of  $F(s)$  are to one side of the line. We can see that both  $P(x, s, t_1)$  and  $Q(s)$  are holomorphic in  $s$ . Thus we have that [15, p. 632]

$$u_0(x, t_0, t_1) = \frac{1}{2\pi i} \int_{\gamma-i\infty}^{\gamma+i\infty} U_0(x, s, t_1)e^{st_0} ds = \frac{1}{2\pi i} \oint U_0(x, s, t_1)e^{st_0} ds \quad (4.25)$$

$$= \sum_n \text{Res}(U_0(x, s, t_1)e^{st_0}, s_n), \quad (4.26)$$

where  $s_n$  are the poles of  $U_0(x, s, t_1)e^{st_0}$  with respect to  $s$ . Since we have that  $U_0(x, s, t_1) = P_0(x, s, t_1)/Q(s)$  the poles are given by the roots of  $Q(s)$ .

#### 4.1.2 Root finding characteristic function: $Q(s)$

From Equation (4.21) we can see that we have a root if  $s = 0$  or if

$$\chi(s) = (\kappa_0 + s)e^{2sL} - \gamma_0 s - \kappa_0 = 0. \quad (4.27)$$

We substitute  $s = \mu_1 + i\mu_2$ , where  $\mu_1, \mu_2 \in \mathbb{R}$ , to obtain that

$$\chi_{re}(\mu_1, \mu_2) = \Re(\chi(\mu_1 + i\mu_2)) = [(\kappa_0 + \mu_1) \cos(2\mu_2 L) - \mu_2 \sin(2\mu_2 L)] e^{2\mu_1 L} - \gamma_0 \mu_1 - \kappa_0 = 0, \quad (4.28)$$

$$\chi_{im}(\mu_1, \mu_2) = \Im(\chi(\mu_1 + i\mu_2)) = [(\kappa_0 + \mu_1) \sin(2\mu_2 L) + \mu_2 \cos(2\mu_2 L)] e^{2\mu_1 L} - \gamma_0 \mu_2 = 0. \quad (4.29)$$

In Figure 9 the lines corresponding to  $\chi_{re} = 0$  and  $\chi_{im} = 0$  are shown for  $\kappa_0 = 1/5$  and  $\gamma_0 = 1/2$ . The roots of the equation are where the two different lines cross. The corresponding equations can not be

solved analytically, and hence the roots must be found numerically. However, we do need to study these equations to obtain good initial guesses and bounds for our numerical schemes.

Let us first consider symmetry in the equation. We can see that

$$\chi_{re}(\mu_1, -\mu_2) = \chi_{re}(\mu_1, \mu_2), \quad (4.30)$$

$$\chi_{im}(\mu_1, -\mu_2) = -\chi_{im}(\mu_1, \mu_2). \quad (4.31)$$

Thus if  $\mu_1 + i\mu_2$  is a root of  $\chi(s)$  then  $\mu_1 - i\mu_2$  is also a root. So we only have to search for poles with  $\mu_2 \geq 0$ .

Now let us consider the case that  $\mu_2 = 0$ . Then we have that  $\chi_{im}(\mu_1, 0) = 0$  and that

$$\chi_{re}(\mu_1, 0) = (\kappa_0 + \mu_1)e^{2\mu_1 L} - \gamma_0\mu_1 - \kappa_0 \quad (4.32)$$

$$= (e^{2\mu_1 L} - 1)\kappa_0 + (e^{2\mu_1 L} - \gamma_0)\mu_1 = 0. \quad (4.33)$$

We can see that we always have a root for  $\mu_1 = 0$ . If  $\mu_1 > 0$ , then we see that both terms are positive so there is no positive root. Using that  $L \gg 1$ , we can see that for  $\mu_1 < 0$ , the exponents vanish and thus we have that the root is approximately at  $\mu_1 = -\kappa_0/\gamma_0$ . Since we have assumed that the springs are extended,  $\kappa_0 > 0$ , this only holds for  $\gamma_0 > 0$ , because we have just shown that  $\mu_1 \leq 0$ . Thus, we do not have the second root if  $\gamma_0 \leq 0$ .

We now consider the behaviour of the whole system. If we look at the structure of the equations, we see that we can write it as a vector equation

$$\boldsymbol{\chi} = \begin{pmatrix} \cos(2\mu_2 L) & -\sin(2\mu_2 L) \\ \sin(2\mu_2 L) & \cos(2\mu_2 L) \end{pmatrix} \begin{pmatrix} \kappa_0 + \mu_1 \\ \mu_2 \end{pmatrix} e^{2\mu_1 L} - \begin{pmatrix} \gamma_0\mu_1 + \kappa_0 \\ \gamma_0\mu_2 \end{pmatrix} = R_{2\mu_2 L} \mathbf{a} - \mathbf{b}, \quad (4.34)$$

where  $R_{2\mu_2 L}$  denotes the rotation matrix. Thus to obtain that  $\boldsymbol{\chi} = \mathbf{0}$  we need that

$$\|\mathbf{a}\| = \|\mathbf{b}\|, \quad (4.35)$$

$$\angle(\mathbf{a}) + 2\mu_2 L - 2k\pi = \angle(\mathbf{b}), \quad (4.36)$$

where  $\angle(\cdot)$  denotes the angle of the vector and  $k \in \mathbb{Z}$ . It follows that

$$\mu_2^2 = \frac{(\gamma_0\mu_1 + \kappa_0)^2 - e^{4\mu_1 L}(\mu_1 + \kappa_0)^2}{e^{4\mu_1 L} - \gamma_0^2} = \frac{f_{num}(\mu_1)}{e^{4\mu_1 L} - \gamma_0^2}, \quad (4.37)$$

$$2\mu_2 L - 2k\pi = \arctan \left[ \frac{\mu_2 \kappa_0 (\gamma_0 - 1)}{(\kappa_0 \mu_1 + \mu_1^2 + \mu_2^2) \gamma_0 + \kappa_0 (\mu_1 + \kappa_0)} \right]. \quad (4.38)$$

From the bottom equation, we can see that there exists an infinite number of solutions  $\mu_{k,2}$  where  $k$  is chosen such that  $-\pi \leq 2\mu_{k,2} L - 2k\pi \leq \pi$ . With Equation (4.37) we can obtain bounds on  $\mu_{k,1}$  since we must have that the right-hand side is positive.

If we have that  $\mu_{k,1} > 0$ , then we know that for the denominator  $e^{4\mu_{k,1} L} - \gamma_0^2 > 0$  holds. However, using that  $e^{4\mu_{k,1} L} > 1$  we obtain for the numerator that

$$f_{num}(\mu_{k,1}) = (\gamma_0\mu_{k,1} + \kappa_0)^2 - e^{4\mu_{k,1} L}(\mu_{k,1} + \kappa_0)^2 < (\gamma_0^2 - 1)\mu_{k,1}^2 + 2\mu_{k,1}\kappa_0(\gamma_0 - 1) \leq 0, \quad (4.39)$$

where we have used that  $\gamma_0 \in [-1, 1)$ . Thus we must have that  $\mu_{k,1} \leq 0$ .

Now, if we consider the numerator,  $f_{num}(\mu_1)$ , we can see that it consists of two parabolas, where the negative one is scaled by the exponent. Since  $L \gg 1$ , the positive parabola dominates away from zero. At  $\mu_1 = 0$  we see that  $f_{num}(0) = 0$  and furthermore we have that

$$f'_{num}(0) = -4 \left( 2\kappa_0 L + \frac{1}{2}(1 - \gamma_0) \right) \kappa_0 < 0. \quad (4.40)$$

So  $f_{num}$  is positive close to zero, where the exponent is not yet negligible, and hence  $f_{num}(\mu_1) \geq 0$  for  $\mu_1 \leq 0$ . Thus we need that  $e^{4\mu_{k,1} L} - \gamma_0^2 > 0$ , which gives us the following bound

$$\frac{\ln(|\gamma_0|)}{2L} < \mu_{k,1} \leq 0. \quad (4.41)$$

Now let us consider the case  $\mu_{k,2} \gg 1$ , then we can see from Equation (4.37) that  $e^{4\mu_{k,1} L} - \gamma_0^2 \ll 1$ , since the numerator is limited by the bound on  $\mu_{k,1}$ . Thus as  $\mu_{k,2}, k \rightarrow \infty$  we have that  $\mu_{k,1} \rightarrow \ln(|\gamma_0|)/(2L)$ .

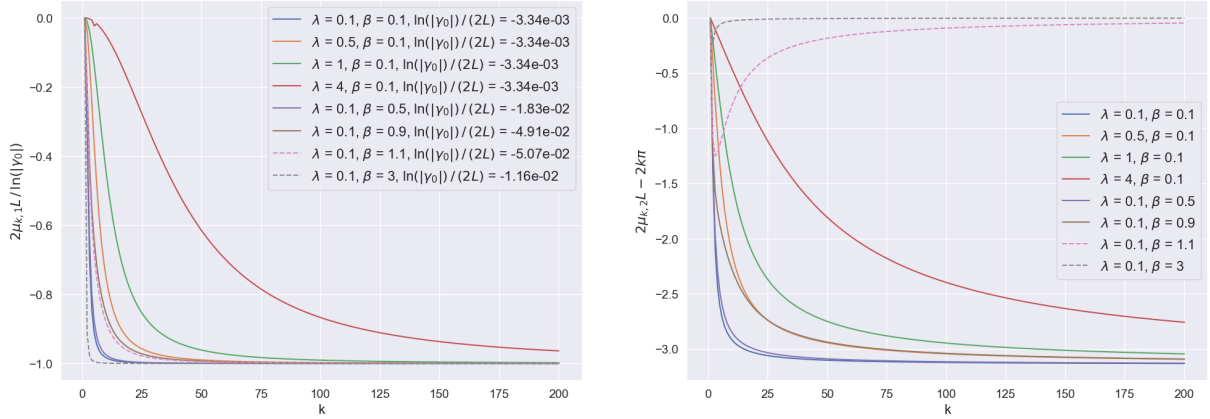


**Figure 10:** Pole locations for different values of  $\lambda$  and  $\beta$ . The real part,  $\mu_{k,1}$ , is normalised by its maximum value  $\ln|\gamma_0|/(2L)$  and the imaginary part,  $\mu_{k,2}$  is shifted by  $2k\pi$ .

So, if we substitute Equation (4.37) into Equation (4.38) to obtain a function only in  $\mu_1$  and solve it numerically. Due to this limit, we have that for larger values of  $k$ , small errors in the solution  $\mu_{k,1}$  will blow up when calculating  $\mu_{k,2}$ .

In Figure 10, the locations of the poles for different values of  $\lambda$  and  $\beta$  are plotted. The real part is normalised by the maximal value  $\ln(|\gamma_0|)/(2L)$  and the imaginary part is shifted by  $2k\pi$ . We can see that as  $k$  increases the real part tends to its maximal value and the imaginary value tends to 0 or  $-\pi$ . The imaginary value converges to  $-\pi$  for  $\beta < 1$ , i.e.  $\gamma_0 < 0$ , and to 0 for  $\beta > 1$ . Furthermore, we see that for larger values of  $\lambda$  the real and imaginary parts converge more slowly towards their respective values.

To find the roots, we will minimise the function  $\chi_{re}^2 + \chi_{im}^2$ . For this, the scipy [16] function, which implements the L-BFGS-B [17], [18] algorithm, was used. As the initial guess for the minimisation problem, we first use one of the crossings with the imaginary axis of  $\chi_{re} = 0$  or  $\chi_{im} = 0$ . In Figure 10, we have seen that as  $k$  becomes larger  $\mu_{k,1}$  will only change slightly and  $\mu_{k,2}$  will not deviate much from its periodic shift. Thus for higher values of  $k$ , we use  $(\mu_{k-1,1}, \mu_{k-1,2} + \frac{\pi}{L})$  as an initial guess. The L-BFGS-B algorithm also makes use of bounds on the parameters. For the bound on  $\mu_{k,1}$  we use Equation (4.41) and for the bound on  $\mu_{k,2}$  we use

$$\mu_{k,2}^{(0)} - \frac{\pi}{L} \leq \mu_{k,2} \leq \mu_{k,2}^{(0)} + \frac{\pi}{L}, \quad (4.42)$$

where  $\mu_{k,2}^{(0)}$  is the initial guess for  $\mu_{k,2}$ .

To determine the crossings with the imaginary axis, we substitute  $\mu_1 = 0$  and obtain the following relations

$$\chi_{re} : [\cos(2\mu_2 L) - 1]\kappa_0 - \mu_2 \sin(2\mu_2 L) = 0, \quad (4.43)$$

$$\chi_{im} : \kappa_0 \sin(2\mu_2 L) + [\cos(2\mu_2 L) - \gamma_0]\mu_2 = 0. \quad (4.44)$$

We can see that the equation from  $\chi_{re}$  is always satisfied for  $\mu_2 = k\pi/L$ ,  $k \in \mathbb{Z}$ . The other imaginary axis crossing can be found if we consider  $\mu_2 \rightarrow \infty$ , then we need that  $\sin(2\mu_2 L) = 0$ . So we have that the crossing is approximately at  $\mu_2 = (k + \frac{1}{2})\pi/L$ . From Equation (4.44) we find the crossings also by considering  $\mu_2 \rightarrow \infty$  as  $\mu_2 = [\cos^{-1}(\gamma_0) + 2k\pi]/(2L)$  and  $\mu_2 = [\cos^{-1}(-\gamma_0) + (2k + 1)\pi]/(2L)$ , where the inverse cosines are well-defined since  $-1 \leq \gamma_0 < 1$ . We take  $\mu_{k,2}^{(0)} = k\pi/L$  as our initial guess for the minimization scheme since that is an analytic solution for  $\chi_{re}$ .

#### 4.1.3 First order solution

With the locations of the poles known, we also need to know the order of the poles. To consider the order we first calculate the derivative of  $\chi(s)$  and we obtain

$$\chi'(s) = [2L(\kappa_0 + s) + 1]e^{2sL} - \gamma_0. \quad (4.45)$$

Since we have that  $L \gg 1$  we see that we have  $\chi'(s) = -\gamma_0$  for  $\Re(s) \leq 0$ . If  $\gamma_0 \neq 0$  then there are no zeros of  $\chi'(s)$  in the left half of the complex plane and thus the zeros of  $\chi(s)$  are first-order zeros. If  $\gamma_0 = 0$ ,

then we have a zero at

$$s = -\kappa_0 - \frac{1}{2L}. \quad (4.46)$$

Because  $\gamma_0 < 1$ , this point does not coincide with the zero at  $(-\kappa_0/\gamma_0, 0)$  and hence we again have that the zeros of  $\chi(s)$  are first-order zeros.

So we have that all non-zero roots,  $s_k$ , of  $\chi(s)$  are simple poles of  $U_0$  and thus we have that

$$\text{Res}(U_0(x, s, t_1)e^{st_0}, s_k) = \text{Res}\left(\frac{P_0(x, s, t_1)}{Q(s)}e^{st_0}, s_k\right) = \frac{P_0(x, s_k, t_1)}{Q'(s_k)}e^{s_k t_0}. \quad (4.47)$$

However, since  $Q(s) = 2s\chi(s)$ , we have that  $s = 0$  is a second-order pole. For the residue of  $s = 0$ , we have

$$\text{Res}(U_0(x, s, t_1)e^{st_0}, 0) = \lim_{s \rightarrow 0} \frac{d}{ds} \frac{s^2 P_0(x, s, t_1)e^{st_0}}{Q(s)} = \lim_{s \rightarrow 0} \frac{d}{ds} \frac{s P_0(x, s, t_1)e^{st_0}}{2\chi(s)} = 0, \quad (4.48)$$

where we obtained the result by applying l'Hôpital's rule two times and using that  $P(x, 0, t_1) = 0$  and  $\frac{d}{ds}P(x, s, t_1)|_{s=0} = 0$ . So we have that

$$u_0(x, t_0, t_1) = \sum_k \frac{P_0(x, s_k, t_1)}{Q'(s_k)} e^{s_k t_0}. \quad (4.49)$$

We can see that the real part of  $s_k$  indicates the amount of damping in the system, and from Equation (4.41), we know that it is always negative or zero; hence, we have a stable system. Furthermore, the amount of damping is limited by a function of  $\gamma_0$  and  $L$ .

Since each  $s_k$  is a root of  $Q(s)$  we can see that

$$e^{2s_k L} = \frac{\kappa_0 + \gamma_0 s_k}{\kappa_0 + s_k}. \quad (4.50)$$

If we substitute the above relation into  $P(x, s_k, t_1)$ , eq. (4.23), it reduces to

$$P_0(x, s_k, t_1) = \left[ e^{s_k x} - \frac{\kappa_0 + \gamma_0 s_k}{\kappa_0 + s_k} e^{-s_k x} \right] \cdot \left[ -(\kappa_0 + s_k) \int_0^L h_0(\xi, s_k, t_1) \left( e^{s_k \xi} - \frac{\kappa_0 + \gamma_0 s_k}{\kappa_0 + s_k} e^{-s_k \xi} \right) d\xi - \frac{2s_k \beta}{\beta + 1} a_0(0, t_1) \right] \quad (4.51)$$

$$= \phi_k(x) A_k(t_1). \quad (4.52)$$

Finally Equation (4.49) becomes

$$u_0(x, t_0, t_1) = \sum_k \frac{\phi_k(x) A_k(t_1)}{Q'(s_k)} e^{s_k t_0} = \sum_k \hat{\phi}_k(x) A_k(t_1) e^{s_k t_0}, \quad (4.53)$$

where we have introduced  $\hat{\phi}_k(x) = \phi_k(x)/Q'(s_k)$ .

It is useful to consider whether  $u_0$  above is real or not, since we are modelling a real process and obtained a sum of complex values. First, we note that we have that  $s_{-k} = \bar{s}_k$ , so we can see that

$$\hat{\phi}_{-k}(x) = \overline{\hat{\phi}_k(x)}, \quad e^{s_{-k} t_0} = \overline{e^{s_k t_0}}. \quad (4.54)$$

Now, if we also have that  $A_{-k} = \overline{A_k}$ , we see that we have the sum of a complex number with its complex conjugate, and thus we have a real result.

#### 4.1.4 Second order; second time scale

We will use the system of the second order, Equation (4.7), to determine the functions  $a_0(x, t_1)$  and  $b_0(x, t_1)$ . However, we first need to make the boundary condition homogeneous. We introduce

$$u_1(x, t_0, t_1) = \nu_1(x, t_0, t_1) + \left(\frac{x}{L} - 1\right) T(t_0, t_1), \quad (4.55)$$

where the function  $T(t_0, t_1)$  is determined by substitution into Equation (4.7b). We want the equation to be homogenous in  $\nu_1$ , thus we have that

$$\beta T_{t_0}(t_0, t_1) + \left(\lambda + \frac{1}{L}\right) T(t_0, t_1) = \left[ \beta u_{0,t_1} + \frac{1}{2} u_{0,x}^3 + \kappa \ell_0 u_0^3 + 2\alpha u_0^2 u_{0,t_0} \right]_{(0,t_0,t_1)} \quad (4.56)$$

$$= \hat{h}(t_0, t_1). \quad (4.57)$$

Now if we assume that  $T(0, 0) = 0$ , then it follows that

$$T(t_0, t_1) = \frac{1}{\beta} e^{-\zeta t_0} \int_0^{t_0} \hat{h}(\tau, t_1) e^{\zeta \tau} d\tau, \quad (4.58)$$

where  $\zeta = (\lambda + 1/L)/\beta$ . Since we have to divide by  $\beta$ , additionally make the assumption  $\beta \neq 0$  for our further analysis. Furthermore, we have to assume that  $\beta = \mathcal{O}(1)$  to maintain the correct ordering.

Now we can see that Equation (4.7) becomes

$$\begin{aligned} \nu_{1,t_0 t_0} = \nu_{1,xx} - \left(\frac{x}{L} - 1\right) \left( \frac{1}{\beta} \hat{h}_{t_0}(t_0, t_1) - \frac{\zeta}{\beta} \hat{h}(t_0, t_1) + \frac{\zeta^2}{\beta} e^{-\zeta t_0} \int_0^{t_0} \hat{h}(\tau, t_1) e^{\zeta \tau} d\tau \right) \\ - 2u_{0,t_0 t_1} + \frac{\Gamma}{2} u_{0,xx} \int_0^L u_{0,x}^2 d\xi, \quad 0 < x < L, \quad t_0, t_1 > 0, \end{aligned} \quad (4.59a)$$

$$\nu_{1,x}(0, t_0, t_1) = \lambda \nu_1(0, t_0, t_1) + \beta \nu_{1,t_0}(0, t_0, t_1), \quad t_0, t_1 > 0, \quad (4.59b)$$

$$\nu_1(L, t_0, t_1) = 0, \quad t_0, t_1 > 0, \quad (4.59c)$$

$$\nu_1(x, 0, 0) = 0, \quad 0 < x < L, \quad (4.59d)$$

$$\nu_{1,t_0}(x, 0, 0) = -u_{0,t_0}(x, 0, 0) - \left(\frac{x}{L} - 1\right) \frac{1}{\beta} \hat{h}(0, 0), \quad 0 < x < L. \quad (4.59e)$$

We will denote the inhomogeneous forcing term in Equation (4.59a) as  $\hat{F}(x, t_0, t_1)$ .

To solve the system, we will again use the Laplace transform and use the same steps as in Section 4.1.1, so we obtain the system

$$V_{1,xx}(x, s, t_1) = s^2 V_1(x, s, t_1) - \left[ h_1(x, s, t_1) - \mathcal{L}\{\hat{F}\}(x, s, t_1) \right], \quad 0 < x < L, \quad s \in \mathbb{C}, \quad t_1 > 0, \quad (4.60a)$$

$$V_{1,x}(0, s, t_1) = (\lambda + \beta s) V_1(0, s, t_1) - \beta a_1(0, t_1), \quad s \in \mathbb{C}, \quad t_1 > 0, \quad (4.60b)$$

$$V_1(L, s, t_1) = 0, \quad s \in \mathbb{C}, \quad t_1 > 0, \quad (4.60c)$$

where we have that  $h_1(x, s, t_1) = sa_1(x, t_1) + b_1(x, t_1)$  with

$$a_1(x, t_1) = \nu_1(x, 0, 0) = 0, \quad b_1(x, t_1) = \nu_{1,t_0}(x, 0, 0) = -u_{0,t_0}(x, 0, 0) - \left(\frac{x}{L} - 1\right) \frac{1}{\beta} \hat{h}(0, 0). \quad (4.61)$$

Now the solution of the system is given by

$$V_1(x, s, t_1) = \frac{P_1(x, s, t_1) - P_{\hat{F}}(x, s, t_1)}{Q(s)}, \quad (4.62)$$

where  $Q(s)$  is the same as Equation (4.21). We have split the numerator in the contribution from  $h_1$  and  $\mathcal{L}(\hat{F})$ , this splitting is possible since  $P_0(x, s, t_1)$  is linear in  $h_0(x, s, t_1)$ . Thus, we have that  $P_1(x, s, t_1)$  is the same as  $P_0(x, s, t_1)$ , eq. (4.23), but with  $h_0$  and  $a_0$  replaced by  $h_1$  and  $a_1$  respectively. Comparably, we have that  $P_{\hat{F}}(x, s, t_1)$  is as  $P_0(x, s, t_1)$  but with  $h_0$  replaced by  $\mathcal{L}(\hat{F})$  and without the  $a_0$  terms.

To obtain  $\nu_1(x, t_0, t_1)$ , we want to apply the inverse Laplace transform again. For the first term  $P_1(x, s, t_1)/Q(s)$ , we can apply the transform as we did for the first order, since it has the same structure. However, for the second term we need to study  $\mathcal{L}(\hat{F})$  in more detail. We have that  $u_0(x, t_0, t_1) = \sum_k \hat{\phi}_k(x) A_k(t_1) e^{s_k t_0}$ , so we can write each term of the forcing also as a sum. In the following, we interchange the infinite sum with differentiation and integration, which is allowed since the function is continuous and since it is a solution of  $u_{0,t_0 t_0} = u_{0,xx}$  it is twice differentiable with respect to  $t_0$  and  $x$  [19]. We have that

$$u_{0,t_0 t_1}(x, t_0, t_1) = \sum_n s_n \hat{\phi}_n(x) A'_n(t_1) e^{s_n t_0}, \quad (4.63)$$

$$u_{0,xx}(x, t_0, t_1) \int_0^L u_{0,x}^2(\xi, t_0, t_1) d\xi = \sum_{ijk} s_i^2 \hat{\phi}_i(x) \Phi_{jk} A_{ijk}(t_1) e^{s_{ijk} t_0}, \quad (4.64)$$

where  $\Phi_{jk} = \int_0^L \hat{\phi}'_j \hat{\phi}'_k d\xi$ ,  $A_{ijk}(t_1) = A_i(t_1)A_j(t_1)A_k(t_1)$  and  $s_{ijk} = s_i + s_j + s_k$ . For the term due to the homogenization of the boundary condition, we first write

$$\hat{h}(t_0, t_1) = \sum_n \beta \hat{\phi}_n(0) A'_n(t_1) e^{s_n t_0} + \sum_{ijk} \Psi_{ijk} A_{ijk}(t_1) e^{s_{ijk} t_0}, \quad (4.65)$$

with  $\Psi_{ijk} = \frac{1}{2} \hat{\phi}'_i(0) \hat{\phi}'_j(0) \hat{\phi}'_k(0) + (\kappa_0 \ell_0 + 2\alpha s_k) \hat{\phi}_i(0) \hat{\phi}_j(0) \hat{\phi}_k(0)$ . Thus, it follows that

$$\begin{aligned} \frac{1}{\beta} \hat{h}_{t_0}(t_0, t_1) - \frac{\zeta}{\beta} \hat{h}(t_0, t_1) + \frac{\zeta^2}{\beta} e^{-\zeta t_0} \int_0^{t_0} \hat{h}(\tau, t_1) e^{\zeta \tau} d\tau &= \sum_n \left[ s_n - \zeta + \frac{\zeta^2}{s_n + \zeta} \right] \hat{\phi}_n(0) A'_n(t_1) e^{s_n t_0} \\ &+ \sum_{ijk} \frac{1}{\beta} \left[ s_{ijk} - \zeta + \frac{\zeta^2}{s_{ijk} + \zeta} \right] \Psi_{ijk} A_{ijk}(t_1) e^{s_{ijk} t_0} \\ &- \frac{\zeta^2}{\beta} e^{-\zeta t_0} \left[ \sum_n \frac{\beta}{s_n + \zeta} \hat{\phi}_n(0) A'_n(t_1) + \sum_{ijk} \frac{1}{s_{ijk} + \zeta} \Psi_{ijk} A_{ijk}(t_1) \right]. \end{aligned} \quad (4.66)$$

Putting it all together, we can see that

$$\hat{F}(x, t_0, t_1) = \sum_n \mathcal{A}_n(x, t_1) e^{s_n t_0} + \sum_{ijk} \mathcal{B}_{ijk}(x, t_1) e^{s_{ijk} t_0} + \mathcal{C}(x, t_1) e^{-\zeta t_0}, \quad (4.67)$$

with

$$\mathcal{A}_n(x, t_1) = \left[ -2s_n \hat{\phi}_n(x) - \left( \frac{x}{L} - 1 \right) \frac{s_n^2}{s_n + \zeta} \hat{\phi}_n(0) \right] A'_n(t_1) = \hat{\mathcal{A}}_n(x) A'_n(t_1), \quad (4.68)$$

$$\mathcal{B}_{ijk}(x, t_1) = \left[ \frac{\Gamma}{2} s_i^2 \hat{\phi}_i(x) \Phi_{jk} - \left( \frac{x}{L} - 1 \right) \frac{s_{ijk}^2}{\beta(s_{ijk} + \zeta)} \Psi_{ijk} \right] A_{ijk}(t_1) = \hat{\mathcal{B}}_{ijk}(x) A_{ijk}(t_1), \quad (4.69)$$

$$\mathcal{C}(x, t_1) = \left( \frac{x}{L} - 1 \right) \frac{\zeta^2}{\beta} \left[ \sum_n \frac{\beta}{s_n + \zeta} \hat{\phi}_n(0) A'_n(t_1) + \sum_{ijk} \frac{1}{s_{ijk} + \zeta} \Psi_{ijk} A_{ijk}(t_1) \right]. \quad (4.70)$$

Taking the Laplace transform we obtain the following

$$\mathcal{L}(\hat{F})(x, s, t_1) = \sum_n \frac{\mathcal{A}_n(x, t_1)}{s - s_n} + \sum_{ijk} \frac{\mathcal{B}_{ijk}(x, t_1)}{s - s_{ijk}} + \frac{\mathcal{C}(t_1)}{s + \zeta}. \quad (4.71)$$

So we can see that  $P_{\hat{F}}(x, s, t_1)$  can be written as

$$P_{\hat{F}}(x, s, t_1) = \sum_n \frac{P_{\mathcal{A}_n}(x, s, t_1)}{s - s_n} + \sum_{ijk} \frac{P_{\mathcal{B}_{ijk}}(x, s, t_1)}{s - s_{ijk}} + \frac{P_{\mathcal{C}}(x, s, t_1)}{s + \zeta}, \quad (4.72)$$

where  $P_{\mathcal{A}_n}(x, s, t_1)$ ,  $P_{\mathcal{B}_{ijk}}(x, s, t_1)$  and  $P_{\mathcal{C}}(x, s, t_1)$  are defined similar to  $P_{\hat{F}}(x, s, t_1)$ . So now we can invert the Laplace transform to obtain

$$\begin{aligned} \nu_1(x, t_0, t_1) &= \sum_m \text{Res} \left( \left\{ \frac{P_1(x, s, t_1)}{Q(s)} - \sum_n \frac{P_{\mathcal{A}_n}(x, s, t_1)}{(s - s_n)Q(s)} - \sum_{ijk} \frac{P_{\mathcal{B}_{ijk}}(x, s, t_1)}{(s - s_{ijk})Q(s)} \right. \right. \\ &\quad \left. \left. - \frac{P_{\mathcal{C}}(x, s, t_1)}{(s + \zeta)Q(s)} \right\} e^{st_0}, s_m \right). \end{aligned} \quad (4.73)$$

If  $m = n$ , we can see that that  $s_m$  is now a second order zero of  $(s - s_n)Q(s)$ , thus the residue then changes into

$$\text{Res} \left( \frac{P_{\mathcal{A}_n}(x, s, t_1) e^{st_0}}{(s - s_n)Q(s)}, s_n \right) = \lim_{s \rightarrow s_n} \frac{d}{ds} \frac{(s - s_n) P_{\mathcal{A}_n}(x, s, t_1) e^{st_0}}{Q(s)} \quad (4.74)$$

$$= \frac{2Q'(s_n)[\partial_s P_{\mathcal{A}_n}(x, s_n, t_1) + t_0 P_{\mathcal{A}_n}(x, s_n, t_1)] - Q''(s_n) P_{\mathcal{A}_n}(x, s_n, t_1)}{2(Q'(s_n))^2} e^{s_n t_0}. \quad (4.75)$$

Here we have a linear  $t_0$  term, which gives the growth observed in [Figure 7](#). Similarly, if there are indices  $m, i, j, k$  such that  $s_m = s_i + s_j + s_k$  or there is an index  $m$  such that  $s_m = -\zeta$ , then we also obtain a linear  $t_0$  term. To remove these growing terms, we will use the freedom given by the second time scale  $t_1$ .

First, we consider if there are resonances with the  $\zeta$  term. We have that  $\zeta = (\lambda + \varepsilon^2)/\beta = \mathcal{O}(1)$  and  $|\Re(s_n)| < |\ln|\gamma_0|/(2L)| = \mathcal{O}(\varepsilon^2)$ . Furthermore, since most  $s_n$  have complex parts, we have that there is no resonance for most indices. If  $\beta > 1$ , we have an the real pole coordinate  $s = -\kappa_0/\gamma_0 = -\lambda/(\beta - 1)$  and as  $\beta$  is chosen to be large then  $s$  becomes smaller. To investigate this, we consider their sum

$$\zeta + s = \frac{\lambda + \varepsilon^2}{\beta} - \frac{\lambda}{\beta} \left( 1 + \frac{1}{\beta} + \frac{1}{\beta^2} + \mathcal{O}\left(\frac{1}{\beta^3}\right) \right) = -\frac{\lambda - \varepsilon^2\beta}{\beta^2} + \mathcal{O}\left(\frac{1}{\beta^3}\right). \quad (4.76)$$

So we can see that this is  $\mathcal{O}(1)$  if  $\beta = \mathcal{O}(1)$  and then the  $\zeta$  term does not produce resonances. If  $\beta$  is larger than  $\mathcal{O}(1/\varepsilon)$ , then the resonances need to be taken into account. However, such a  $\beta$  would violate our ordering, so it is excluded.

We now consider the linear and cubic terms. We treat the different cases where the cubic terms do and do not contribute to the resonances separately. Since we have that for all poles  $\Re(s_n) < 0$ , for small values of  $n$ , the cubic terms do not result in resonances. For example, the real part of  $s_1$ , which is the smallest, cannot equal any combination of three other real parts. Thus we only need to eliminate the linear term  $P_{A_n}$  by setting

$$0 = P_{A_n}(x, s_n, t_1) = -\phi_n(x)(\kappa_0 + s_n) \int_0^L \hat{\mathcal{A}}_n(\xi) A'_n(t_1) \phi_n(\xi) d\xi, \quad (4.77)$$

where we can use the reduced form, [Equation \(4.51\)](#), since  $s_n$  is a pole. It follows that we must have that  $A'_n(t_1) = 0$  and hence  $A_n$  is constant in  $t_1$ . We have that

$$A_n = A_n(0) = -(\kappa_0 + s_n) \int_0^L h_0(\xi, s_n, 0) \phi_n(\xi) d\xi - 2s_n \frac{\beta}{\beta + 1} a_0(0, 0) \quad (4.78)$$

$$= -(\kappa_0 + s_n) \int_0^L (s_n f(\xi) + g(\xi)) \phi_n(\xi) d\xi - 2s_n \frac{\beta}{\beta + 1} f(0). \quad (4.79)$$

Now we consider the first index  $\hat{n}$  such that  $s_{\hat{n}} = s_i + s_j + s_k$ . We know that  $|i|, |j|, |k| < |\hat{n}|$ , thus as shown above we have that  $A_i, A_j$  and  $A_k$  are constant. We introduce

$$\hat{\mathcal{B}}_{(ijk)} = \hat{\mathcal{B}}_{ijk} + \hat{\mathcal{B}}_{ikj} + \hat{\mathcal{B}}_{jik} + \hat{\mathcal{B}}_{jki} + \hat{\mathcal{B}}_{kij} + \hat{\mathcal{B}}_{kji}, \quad (4.80)$$

because the expression of  $\hat{\mathcal{B}}_{ijk}$  depends on the order of the indices, however, the sum  $s_i + s_j + s_k$  does not. To remove the secular terms, we impose that

$$0 = P_{A_{\hat{n}}}(x, s_{\hat{n}}, t_1) + P_{\mathcal{B}_{(ijk)}}(x, s_{\hat{n}}, t_1) \quad (4.81)$$

$$= -(\kappa_0 + s_{\hat{n}}) \phi_{\hat{n}}(x) \left[ \int_0^L \hat{\mathcal{A}}_{\hat{n}}(\xi) A'_{\hat{n}}(t_1) \phi_{\hat{n}}(\xi) d\xi + \int_0^L \hat{\mathcal{B}}_{(ijk)}(\xi) A_{ijk} \phi_{\hat{n}}(\xi) d\xi \right]. \quad (4.82)$$

Since the second integral is independent of  $t_1$ , we can rearrange and integrate to obtain

$$A_{\hat{n}}(t_1) = -\frac{\int_0^L \hat{\mathcal{B}}_{(ijk)}(\xi) \phi_{\hat{n}}(\xi) d\xi}{\int_0^L \hat{\mathcal{A}}_{\hat{n}}(\xi) \phi_{\hat{n}}(\xi) d\xi} A_{ijk} \cdot t_1 - (\kappa_0 + s_{\hat{n}}) \int_0^L (s_{\hat{n}} f(\xi) + g(\xi)) \phi_{\hat{n}}(\xi) d\xi - 2s_{\hat{n}} \frac{\beta}{\beta + 1} f(0). \quad (4.83)$$

Consequently, for the next index  $m$  such that  $s_m = s_{\hat{n}} + s_{i'} + s_{j'}$  becomes a polynomial of  $t_1$  with order 2. This will continue until there are no resonances left, and then every  $A_n(t_1)$  is a polynomial of  $t_1$ . Since the imaginary part increases linearly with  $n$ , eventually for higher values of  $n$  one would also need high values of  $i, j$  and  $k$  to equal the imaginary part. However, the real part of the poles is bounded by  $\ln(|\gamma_0|)/(2L)$ , and thus we would have that  $\Re(s_i + s_j + s_k) > \ln(|\gamma_0|)/(2L)$ . So for higher values of  $k$ , there are eventually no resonances anymore.

The coefficients  $A_n(t_1)$  are finally a polynomial in  $t_1$ . Because  $t_1 = \varepsilon^2 t$ , these solutions will stay bounded for a timescale of  $t = \mathcal{O}\left(\frac{1}{\varepsilon^2}\right)$ .

Now let us consider the complex conjugate of  $A_n(t_1)$ . In the case where there are no cubic resonances, [eq. \(4.79\)](#), it is clear that  $A_{-n}(t_1) = \overline{A_n(t_1)}$ . When there are cubic resonances, we first note that if  $s_{\hat{n}} = s_i + s_j + s_k$  for some  $\hat{n}, i, j, k$ , then we also have that  $s_{-\hat{n}} = s_{-i} + s_{-j} + s_{-k}$ . We can see that

$$\hat{\mathcal{A}}_{-\hat{n}}(t_1) = \overline{\hat{\mathcal{A}}_{\hat{n}}(t_1)}, \quad \hat{\mathcal{B}}_{(-i-j-k)}(t_1) = \overline{\hat{\mathcal{B}}_{(ijk)}(t_1)}. \quad (4.84)$$

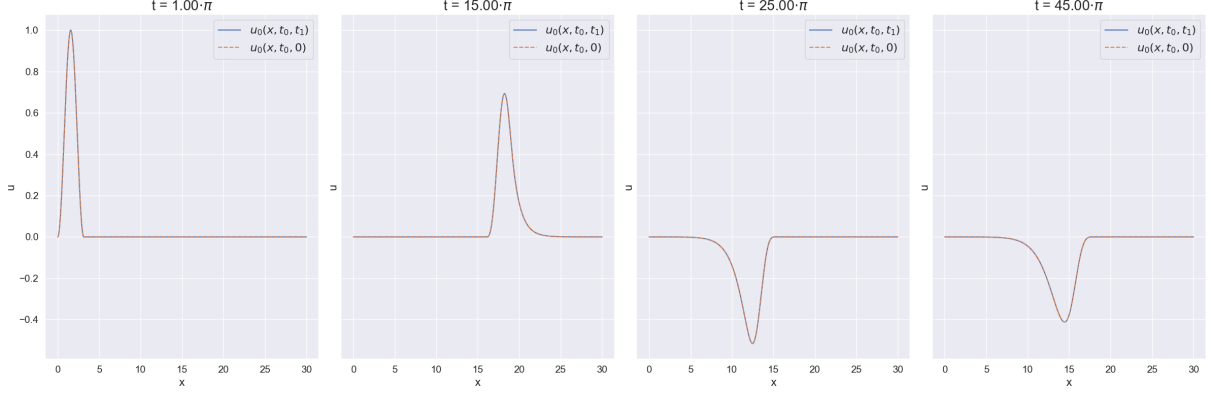


**Figure 11:** Multiple time scale solution for  $\kappa = 2$ ,  $\beta = 0.9$ ,  $\ell_0 = 1/2$  and  $\alpha = 1$ .

Finally, since we have that for the lower values of  $n$  we have that  $\overline{A_{-n}(t_1)} = \overline{A_n(t_1)}$ , we can inductively show that  $A_{-i-j-k}(t_1) = \overline{A_{ijk}(t_1)}$ . Thus we have that  $A_{-n}(t_1) = \overline{A_n(t_1)}$  for all  $n$  and thus we obtain a real solution  $u_0(x, t_0, t_1)$ .

In [Figure 11](#) the multiple time scale solution is plotted for  $\kappa = 2$ ,  $\beta = 0.9$ ,  $\ell_0 = 1/2$  and  $\alpha = 1$ . In the plots, we have also shown the solution with  $t_1 = 0$ , since this corresponds with the  $u_0$  solution in the case of a regular perturbation. We have shown the plots for the times  $t = \pi, 15\pi, 25\pi, 45\pi$ . In the figure, we can see that there is no visible difference between the two solutions, even for the larger times.

To further investigate this, we have plotted the logarithm of the coefficients of the polynomials  $A_n(t_1) = \sum_{i \geq 0} c_i^{(n)} t_1^i$  in [Figure 12](#). First, we see that there are indeed no resonances and no coefficients other than the constant coefficient for small and large  $n$ . When resonances are present, we see that they are only present in certain bands, where the bands have more coefficients for higher values of  $n$ . This is due to the cubic multiplication with the previous terms. Furthermore, we can see that the constant terms and linear terms all have a magnitude of order  $\mathcal{O}(1)$ , however, for higher orders, we see that the order of magnitude drops fast; for  $i = 5$  we already have an order of  $\mathcal{O}(10^{-10})$ . So the contribution of the second time scale is minimal. Hence, we see that the nonlinearity in the case of the extended springs is not significant for larger time scales.

## 4.2 Compressed oblique springs

### 4.2.1 Unstable region

Now we will consider the case where the oblique springs are compressed,  $\ell_0 > 1$ . We again restrict ourselves to the case  $\lambda < 0$  and  $|\lambda| = \mathcal{O}(\varepsilon^2)$ . We assume that

$$\ell_0 = 1 + \rho\varepsilon^2, \quad (4.85)$$

with  $\rho > 0$  and  $\mathcal{O}(\rho) = 1$ . It follows that  $\lambda = -\hat{\lambda}\varepsilon^2$  with  $\hat{\lambda} = 2\kappa\rho$ . As in [Section 3.2](#), the outward force of the springs is shifted to the second order. Thus after using the Laplace transform, we obtain the same system as [Equation \(4.15\)](#) but with  $\lambda = 0$ . As the solution, we have that

$$U_0(x, s, t_1) = \frac{P_{compr}(x, s, t_1)}{Q_{compr}(s)}, \quad (4.86)$$

$$Q_{compr}(s) = 2s [e^{2sL} - \gamma_0], \quad (4.87)$$

$$\begin{aligned} P_{compr}(x, s, t_1) = & \left[ -\gamma_0 \int_0^L h_0(\xi, s, t_1) e^{-\xi s} d\xi + \int_0^x h_0(\xi, s, t_1) e^{\xi s} d\xi + \frac{2\beta}{\beta+1} a_0(0, t_1) \right] e^{s(2L-x)} \\ & + \gamma_0 e^{sx} \int_0^x h_0(\xi, s, t_1) e^{-\xi s} d\xi + e^{s(2L+x)} \int_x^L h_0(\xi, s, t_1) e^{-\xi s} d\xi \\ & + \gamma_0 e^{-sx} \int_x^L h_0(\xi, s, t_1) e^{\xi s} d\xi - \left[ \int_0^L h_0(\xi, s, t_1) e^{\xi s} d\xi + \frac{2\beta}{\beta+1} a_0(0, t_1) \right] e^{sx}. \end{aligned} \quad (4.88)$$

Now we need to find the roots  $s_k$  of  $Q_{compr}(s)$ , which are given by  $s^{(0)} = 0$  and  $e^{2s_k L} = \gamma_0$ . We can see that for  $\gamma_0 = 0$ , there are no other roots except for  $s^{(0)} = 0$ . If we have that  $\gamma_0 \neq 0$  and consequently

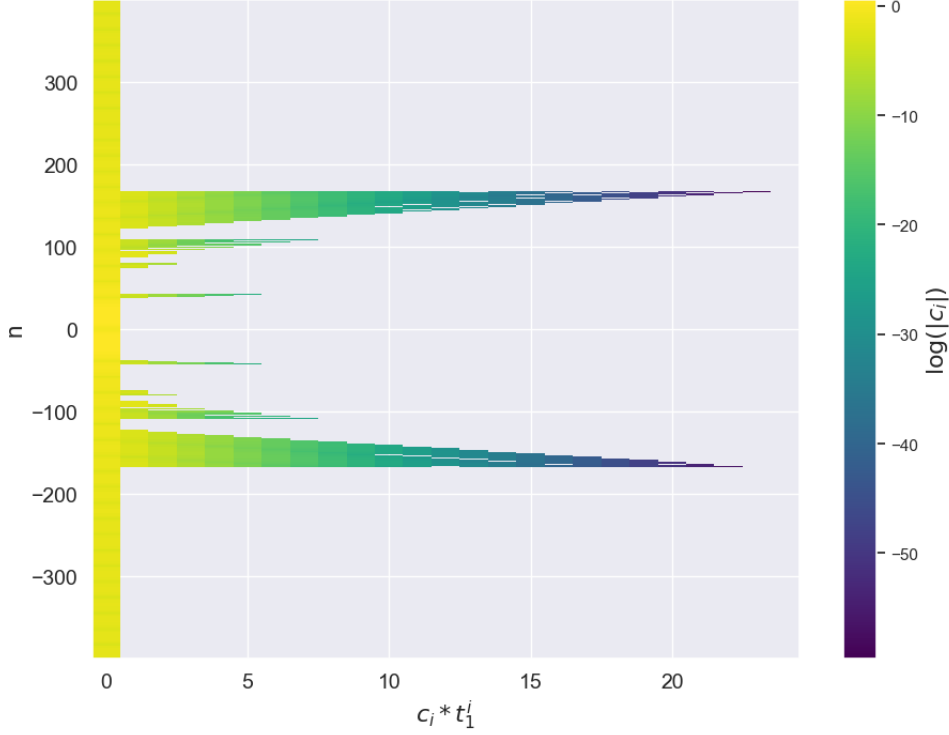


**Figure 12:** Plot of the magnitude of the logarithm of the coefficients of the polynomials  $A_n(t_1) = \sum_{i \geq 0} c_i^{(n)} t_1^i$ .

$\beta \neq 1$ , then we again denote  $s_k = \mu_{k,1} + i\mu_{k,2}$ , and we can see that for the real part we have that

$$\mu_{k,1} = \frac{\ln(|\gamma_0|)}{2L}. \quad (4.89)$$

For the imaginary part we must have that  $e^{2\mu_{k,2}L} = \text{sign}(\gamma_0)$ , thus it follows that

$$\mu_{k,2} = \begin{cases} \frac{k\pi}{L} & \text{if } \gamma_0 > 0, \\ \frac{(2k+1)\pi}{2L} & \text{if } \gamma_0 < 0. \end{cases} \quad (4.90)$$

We can see that

$$P_{compr}(x, s^{(0)}, t_1) = P_{compr}(x, 0, t_1) = 0, \quad (4.91)$$

$$P_{compr}(x, s_k, t_1) = [e^{s_k x} - \gamma_0 e^{-s_k x}] \cdot \left[ -\int_0^L h_0(\xi, s_k, t_1) (e^{s_k \xi} - \gamma_0 e^{-s_k \xi}) d\xi - 2\frac{\beta}{\beta+1} a_0(0, t_1) \right] \quad (4.92)$$

$$= \varphi_k(x) B_k(t_1). \quad (4.93)$$

Now we can again apply the residue theorem to obtain  $u_0(x, t_0, t_1)$ , so we need to calculate the residues. We now have that the pole  $s^{(0)} = 0$  is a first order pole, so we calculate the residue as

$$\text{Res} \left( \frac{P_{compr}(x, s, t_1)}{Q_{compr}(s)} e^{st_0}, 0 \right) = \lim_{s \rightarrow 0} \frac{s P_{compr}(x, s, t_1)}{Q_{compr}(s)} e^{st_0} = \lim_{s \rightarrow 0} \frac{P_{compr}(x, s, t_1)}{2(e^{2sL} - \gamma_0)} e^{st_0} = 0. \quad (4.94)$$

Thus, we can see that we again have that the zero-value pole has no contribution. So, when we have  $\gamma_0 = 0$ , we obtain only the zero solution, and we have perfect damping. The other poles,  $s_k$ , are also first order poles, but they cannot be factored out thus, we have that

$$\text{Res} \left( \frac{P_{compr}(x, s, t_1)}{Q_{compr}(s)} e^{st_0}, s_k \right) = \frac{P_{compr}(x, s_k, t_1)}{Q'_{compr}(s_k)} e^{s_k t_0} = \frac{\varphi_k(x)}{Q'_{compr}(s)} B_k(t_1) e^{s_k t_0} = \hat{\varphi}_k(x) B_k(t_1) e^{s_k t_0}, \quad (4.95)$$

where we have defined  $\hat{\varphi}_k(x) = \varphi_k(x)/Q'_{\text{compr}}(s_k)$ . Finally, we obtain

$$u_0(x, t_0, t_1) = \sum_k \hat{\varphi}_k(x) B_k(t_1) e^{s_k t_0}. \quad (4.96)$$

**Second time scale** We will use the second time scale to determine  $B_k(t_1)$ . After making the boundary condition in the second-order system homogeneous, we obtain the same system as Equation (4.59) but with  $\lambda = 0$ ,  $\zeta$  replaced by  $\hat{\zeta} = 1/(\beta L) = \varepsilon^2/\beta$  and  $\hat{h}(t_0, t_1)$  replaced by

$$\hat{h}_{\text{compr}}(t_0, t_1) = \left[ -\hat{\lambda} u_0 + \beta u_{0,t_1} + \frac{1}{2} u_{0,x}^3 + \kappa \ell_0 u_0^3 + 2\alpha u_0^2 u_{0,t_0} \right]_{(0,t_0,t_1)}. \quad (4.97)$$

Now we need to identify the resonances that occur in the second order. First, we see that the real part of each  $s_k$  is constant in  $k$ , so the cubic terms will not introduce resonances. Resonances can also be created from the  $\hat{\zeta} = \varepsilon^2/\beta$  term. We only a real pole coordinate if  $\beta > 1$ , so then we can have the resonance with  $s_0 = \varepsilon^2 \ln |\gamma_0|/2$ . We consider their sum

$$\frac{s_0 + \hat{\zeta}}{\varepsilon^2} = \frac{1}{2} \ln \left( 1 - \frac{1}{\beta} \right) - \frac{1}{2} \ln \left( 1 + \frac{1}{\beta} \right) + \frac{1}{\beta} \quad (4.98)$$

$$= \frac{1}{2} \left( -\frac{1}{\beta} - \frac{1}{2\beta^2} - \frac{1}{3\beta^3} + \mathcal{O} \left( \frac{1}{\beta^4} \right) \right) - \frac{1}{2} \left( \frac{1}{\beta} - \frac{1}{2\beta^2} + \frac{1}{3\beta^3} + \mathcal{O} \left( \frac{1}{\beta^4} \right) \right) + \frac{1}{\beta} \quad (4.99)$$

$$= -\frac{1}{3\beta^3} + \mathcal{O} \left( \frac{1}{\beta^4} \right). \quad (4.100)$$

So we do have to take this into account if  $\beta = \mathcal{O}(1/\varepsilon^{2/3})$ . For example, in our case where we have  $L = 30$ , this would mean that there is resonance if  $\beta \approx 3.11$ .

We have that

$$\hat{h}_{\text{compr}}(t_0, t_1) = \sum_n \left[ -\hat{\lambda} B_n(t_1) + \beta B'_n(t_1) \right] \hat{\varphi}_n(0) e^{s_n t_0} + \sum_{ijk} [\dots], \quad (4.101)$$

where we have omitted the precise expressions for the cubic terms for conciseness, since there are no resonances with those terms. It follows that

$$\begin{aligned} \frac{1}{\beta} \hat{h}_{\text{compr},t_0}(t_0, t_1) - \frac{\hat{\zeta}}{\beta} \hat{h}_{\text{compr}}(t_0, t_1) + \frac{\hat{\zeta}^2}{\beta} e^{-\hat{\zeta} t_0} \int_0^{t_0} \hat{h}_{\text{compr}}(\tau, t_1) e^{\hat{\zeta} \tau} d\tau = \\ \sum_n \frac{s_n^2}{\beta(s_n + \hat{\zeta})} \left[ -\hat{\lambda} B_n(t_1) + \beta B'_n(t_1) \right] \hat{\varphi}_n(0) e^{s_n t_0} + \sum_{ijk} [\dots] \\ - \hat{\zeta}^2 e^{-\hat{\zeta} t_0} \left[ \sum_n \frac{1}{s_n + \hat{\zeta}} \hat{\varphi}_n(0) B'_n(t_1) + \sum_{ijk} \frac{\Psi_{ijk}}{\beta(s_{ijk} + \hat{\zeta})} B_{ijk}(t_1) \right]. \end{aligned} \quad (4.102)$$

First, we only consider the resonances due to the linear terms. Then with the  $-2u_{0,t_0,t_1}$  term taken into account and doing the same steps as in Section 4.1.4, we obtain that

$$\begin{aligned} \int_0^L \left[ 2s_n \varphi_n(x) \hat{\varphi}_n(x) + \left( \frac{x}{L} - 1 \right) \varphi_n(x) \frac{s_n^2}{s_n + \hat{\zeta}} \hat{\varphi}_n(0) \right] dx \cdot B'_n(t_1) = \\ \int_0^L \left( \frac{x}{L} - 1 \right) \varphi_n(x) dx \hat{\varphi}_n(0) \frac{s_n^2}{\beta(s_n + \hat{\zeta})} \hat{\lambda} B_n(t_1). \end{aligned} \quad (4.103)$$

Finally, we have that

$$B_n(t_1) = C_n e^{Z_n \hat{\lambda} t_1}, \quad (4.104)$$

with

$$Z_n = \frac{\frac{s_n^2}{\beta(s_n + \hat{\zeta})} \varphi_n(0) \int_0^L \left( \frac{x}{L} - 1 \right) \varphi_n(x) dx}{2s_n \int_0^L \varphi_n^2(x) dx + \frac{s_n^2}{s_n + \hat{\zeta}} \varphi_n(0) \int_0^L \left( \frac{x}{L} - 1 \right) \varphi_n(x) dx} \quad (4.105)$$

$$= \frac{-1}{(\beta^2 - 1) s_n L}. \quad (4.106)$$

and with  $C_n$  the initial condition i.e.

$$C_n = - \int_0^L (s_n f(x) + g(x)) \varphi_n(x) dx - 2 \frac{\beta}{\beta + 1} f(0). \quad (4.107)$$

Now let us consider the fraction  $Z_n$ . First we note that  $s_n L = \frac{1}{2} [\ln(|\gamma_0|) + i(2n + \mathbb{1}_{\{\gamma_0 < 0\}})]$ , so we have that  $\Re(s_n L) < 0$  and  $\Re(s_n L) = \mathcal{O}(1)$  if  $\gamma_0$  is not close to zero. We can see that  $\Re(Z_n) > 0$  for  $\beta > 1$  and thus the solution is unstable as we would expect. Furthermore, we can see that the fraction is only dependent on  $\beta$  and  $n$ ; thus, if  $\beta$  is large, then  $Z_n$  will be small and the contribution of the second time scale will be only visible at a larger time. Conversely, since  $\hat{\lambda} = 2\kappa\rho$ , we have that if  $\kappa$  or  $\rho$  becomes larger, then the effects of the second time scale will be visible at a shorter time. However, if  $\beta < 1$ , then  $\Re(Z_n) < 0$  and the solution is stable. If we take  $\beta \rightarrow 0$ , we see that  $\Re(Z_n) \rightarrow 0$  and thus we only have an imaginary contribution of the second time scale. This behaviour is caused by the multiple time scale method.

To understand this, we consider the linearization of the left boundary conditions, we have

$$u_x(0, t) = \beta u_t(0, t) - \varepsilon^2 \hat{\lambda} u(0, t). \quad (4.108)$$

Now we will solve this without delegating the outward force to the second order. Then we obtain a characteristic function as Equation (4.27) with  $\kappa_0$  replaced by  $-\varepsilon^2 \hat{\kappa}_0$ , where  $\hat{\kappa}_0 = \hat{\lambda}/(\beta + 1)$ . So we have

$$\hat{\chi}(s) = (s - \varepsilon^2 \hat{\kappa}_0) e^{2sL} - \gamma_0 s + \varepsilon^2 \hat{\kappa}_0 = 0. \quad (4.109)$$

We want to determine the roots,  $s = \mu_1 + i\mu_2$ , of this equation with positive real part,  $\mu_1 > 0$ . Using the vector equation, we again obtain that

$$(e^{4\mu_1 L} - \gamma_0^2) \mu_2^2 + e^{4\mu_1 L} (\mu_1 - \varepsilon^2 \hat{\kappa}_0)^2 = (\gamma_0 \mu_1 - \varepsilon^2 \hat{\kappa}_0)^2. \quad (4.110)$$

Here we can see that if  $\mu_2 \gg 1$ , the equation has no solution. Furthermore, considering the shape of the contours in Figure 9, we can assume that there are no solutions with  $\mu_1 > 0$  and  $\mu_2 \neq 0$ .

So we turn to solutions with  $\mu_2 = 0$ , then we must have that

$$\hat{\chi}(\mu_1) = (\mu_1 - \varepsilon^2 \hat{\kappa}_0) e^{2\mu_1 L} - \gamma_0 \mu_1 + \varepsilon^2 \hat{\kappa}_0 = 0. \quad (4.111)$$

First, we note that  $\mu_1 = 0$  is a solution. To find the other solutions, we determine the derivative, which is

$$\hat{\chi}'(\mu_1) = (2L(\mu_1 - \varepsilon^2 \hat{\kappa}_0) + 1) e^{2\mu_1 L} - \gamma_0. \quad (4.112)$$

We can see that if  $\hat{\chi}'(0) = 1 - 2\hat{\kappa}_0 - \gamma_0$  which is negative if  $\hat{\kappa}_0 > 1$ . Since  $\hat{\kappa}_0 = 2\kappa\rho/(\beta + 1)$  and both  $\kappa$  and  $\rho$  are of  $\mathcal{O}(1)$ , this is reasonable to assume. Now if  $\mu_1 \gg 1$ , then we see that  $\hat{\chi}'(\mu_1) > 0$  and thus we have a positive root. Additionally, if  $\mu_1 \ll -1$ , then  $\hat{\chi}'(\mu_1) \approx -\gamma_0$  and thus we have a negative root if  $\gamma_0 < 0$ .

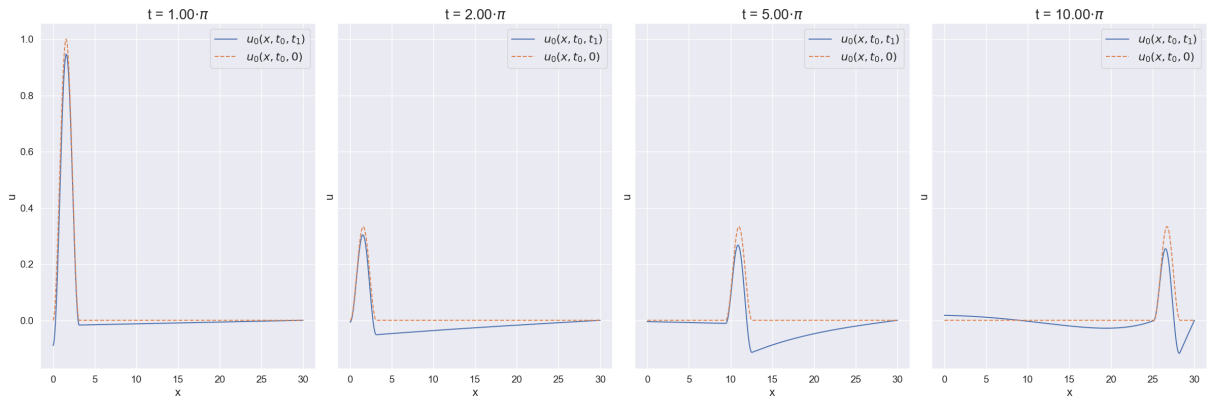
When we delegated the outward force to the second order, we obtained the roots  $\mu_1 = 0$  and, if  $\gamma_0 > 0$ ,  $\mu_1 = \varepsilon^2 \ln |\gamma_0|/2$ . Thus, in our approximation, we find only one root instead of three if  $\gamma_0 < 0$ . If  $\gamma_0 > 0$ , then we find a positive root instead of a negative one. So we have a singular perturbed problem, and from the behaviour of  $Z_n$ , we can see that our multiple time scale method can capture the correct dynamics if  $\gamma_0 > 0$ . However, in the other case, the method cannot be corrected to the right roots, and we unexpectedly obtain a stable solution.

We still need to calculate the value for  $\beta = \mathcal{O}(1/\varepsilon^{2/3})$  and  $n = 0$ . In this case, we also need to take into account the  $e^{-\hat{\zeta}t_0}$  term in Equation (4.102). However, since  $\hat{\zeta} = \varepsilon^2/\beta$ , all the terms in the sums except for  $n = 0$  are of order  $\mathcal{O}(\varepsilon^2)$  or smaller. Thus, the growth of those terms can be neglected, and we only need to take the  $n = 0$  term into account. Then we obtain that

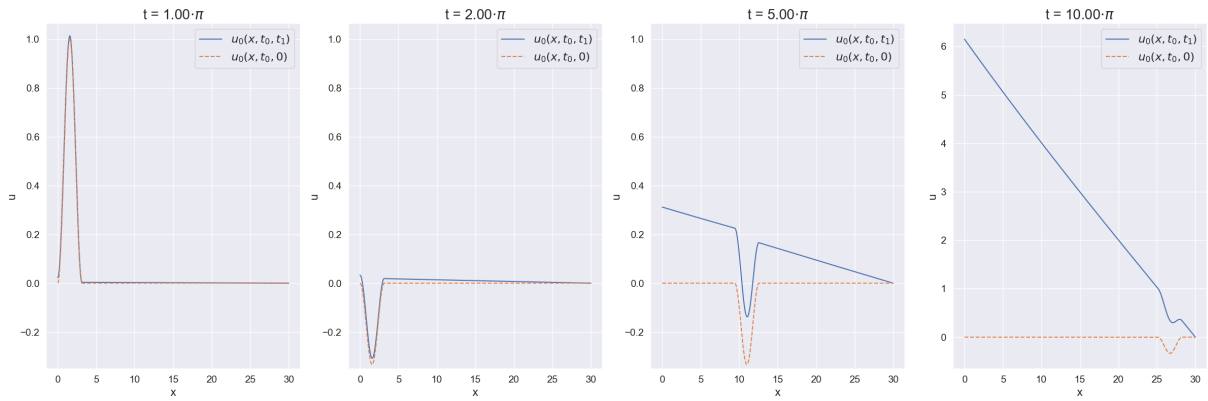
$$\begin{aligned} \int_0^L \left[ 2s_0 \varphi_0(x) \hat{\varphi}_0(x) + \left( \frac{x}{L} - 1 \right) \varphi_0(x) (s_0 - \hat{\zeta}) \hat{\varphi}_0(0) \right] dx \cdot B'_0(t_1) = \\ \int_0^L \left( \frac{x}{L} - 1 \right) \varphi_0(x) dx \hat{\varphi}_0(0) \frac{s_0^2}{\beta(s_0 + \hat{\zeta})} \hat{\lambda} B_0(t_1). \end{aligned} \quad (4.113)$$

Finally, we have that

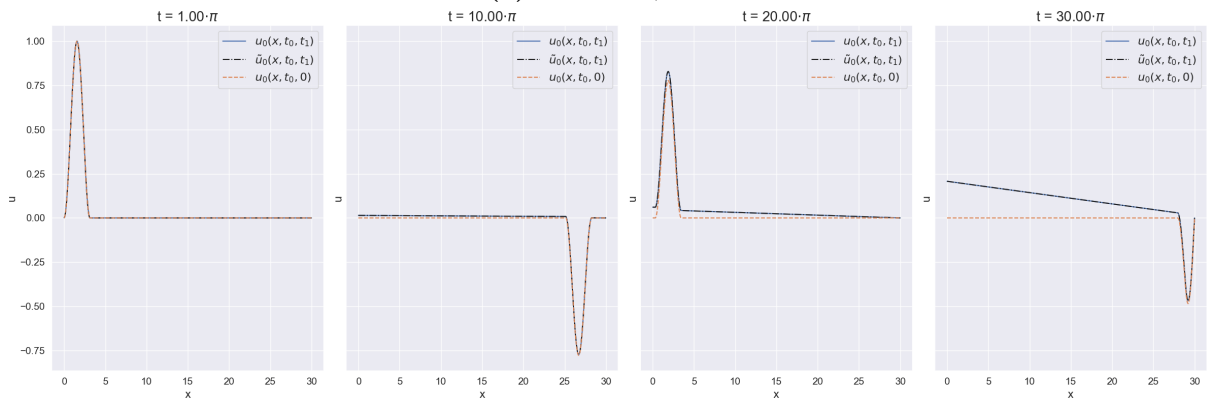
$$Z'_0 = - \frac{\beta s_0^2 L^2}{1 + \beta(\beta^2 - 1) s_0^3 L^3} = - \frac{2\beta \ln^2 |\gamma_0|}{8 + \beta(\beta^2 - 1) \ln^3 |\gamma_0|} \approx - \frac{2\beta}{7\beta^2 + 1}, \quad (4.114)$$



(a) Plots with  $\beta = 1/2$ .



(b) Plots with  $\beta = 2$ .



(c) Plots with  $\beta = 8$ , where  $\tilde{u}_0(x, t_0, t_1)$  is the solution without the modified  $Z_0$ .

**Figure 13:** Plots of the multiple time scale solution for  $\kappa = 2$  and  $\rho = 2.5$  and different values of  $\beta$ .

where we used that  $\ln |\gamma_0| \approx -1/\beta$ . So we can see that the  $n = 0$  term becomes stable.

In Figure 13, we have plotted the solution with different values of  $\beta$  for multiple times. For the other parameters, we have chosen  $\kappa = 2$  and  $\rho = 2.5$ . First, we have shown  $\beta = 1/2$ , to consider the case  $\beta < 1$  in Figure 13a. We can see that the solution stays bounded, and it has oscillations outside of the wave packet, due to the second time scale. Furthermore, we can see that at  $t = \pi$  just before the collision with the boundary, the multiple time scale solution already differs from the first order solution. This is because  $|\Re(Z_n)| > 1$  and it is large enough that the second time scale has a significant contribution before the collision happens. This problem can be mitigated by letting the initial condition start at the boundary.

In Figure 13b, we have plotted the solution with  $\beta = 2$ . In the plots, we can see the unstable behaviour of the system, where the boundary is slowly pushed out of its unstable equilibrium point and keeps growing. Additionally, we have also shown the solution with  $\beta = 8$  in Figure 13c, to investigate the change in  $Z_0$ . In the plot we have added  $\tilde{u}_0(x, t_0, t_1)$  for which  $Z'_0$  was not adjusted. We can see that there is no visible difference between the two solutions, and thus the resonance due to the  $\hat{\zeta}$  term is not strong.

#### 4.2.2 Stable region

The instability in Figure 13b is since we have expanded the forces of the boundary around the unstable equilibrium point,  $u = 0$ . So the stable behaviour is not captured in the model. Thus, we need to split the solution into a stable and unstable domain, where we expand the solution around the stable solution  $u_{eq}(x)$  in the stable domain. We recall that the  $u_{eq}(x) = m(1 - x/L)$ , with  $m$  given by, eq. (3.37),

$$m^2 = \frac{1}{\varepsilon^2}(\ell_{eq}^2 - 1), \quad \ell_{eq} = \frac{\ell_0}{1 + \frac{1}{2\kappa L}}. \quad (4.115)$$

First, we consider the case when the unstable solutions grow towards the upper stable solution. We introduce

$$Y(x, t) = u(x, t) - u_{eq}(x). \quad (4.116)$$

Then the wave equation becomes

$$Y_{tt}(x, t) = Y_{xx}(x, t) + \frac{\varepsilon^2 \Gamma}{2} Y_{xx}(x, t) \left( \int_0^L Y_x^2(\xi, t) d\xi - \varepsilon \sqrt{\ell_{eq}^2 - 1} \int_0^L Y_x(\xi, t) d\xi + \ell_{eq}^2 - 1 \right). \quad (4.117)$$

We can see that this introduces odd orders of  $\varepsilon$  into our equation; however, later we will use the assumption on  $\ell_0$  to simplify things. But first, we also expand the forces on the boundary

$$F_T = \frac{u_x(0, t)}{\sqrt{1 + \varepsilon^2 u_x^2(0, t)}}, \quad F_s = 2\kappa u(0, t) \left[ 1 - \frac{\ell_0}{\sqrt{1 + \varepsilon^2 u^2(0, t)}} \right], \quad F_d = 2\alpha \frac{\varepsilon^2 u^2(0, t)}{1 + \varepsilon^2 u^2(0, t)} u_t(0, t). \quad (4.118)$$

We apply a Taylor expansion of the above formulas around  $u_{eq}(x)$ , so then we obtain

$$F_T = -\frac{\varepsilon^2 m}{\sqrt{1 + \varepsilon^6 m^2}} + \frac{1}{(1 + \varepsilon^6 m^2)^{\frac{3}{2}}} Y_x(0, t) + \frac{3}{2} \frac{\varepsilon^3 m}{(1 + \varepsilon^6 m^2)^{\frac{5}{2}}} \varepsilon Y_x^2(0, t) + \frac{12\varepsilon^6 m^2 - 3}{6(1 + \varepsilon^6 m^2)^{\frac{7}{2}}} \varepsilon^2 Y_x^3(0, t), \quad (4.119)$$

$$F_s = 2\kappa m \left( 1 - \frac{\ell_0}{\ell_{eq}} \right) + 2\kappa \left( 1 - \frac{\ell_0}{\ell_{eq}^3} \right) Y(0, t) + 3\kappa \ell_0 \frac{\sqrt{\ell_{eq}^2 - 1}}{\ell_{eq}^5} \varepsilon Y^2(0, t) - \kappa \ell_0 \frac{4\ell_{eq}^2 - 5}{\ell_{eq}^7} \varepsilon^2 Y^3(0, t), \quad (4.120)$$

$$F_d = 2\alpha Y_t(0, t) \left[ 1 - \frac{1}{\ell_{eq}^2} + 2 \frac{\sqrt{\ell_{eq}^2 - 1}}{\ell_{eq}^4} \varepsilon Y(0, t) + \frac{5 - 3\ell_{eq}^2}{\ell_{eq}^6} \varepsilon^2 Y^2(0, t) \right]. \quad (4.121)$$

Now, to simplify these expressions, we will use the assumption that  $\ell_0 = 1 + \rho\varepsilon^2$ . Then, for example, we can see that

$$\ell_{eq} = \frac{\ell_0}{1 + \frac{1}{2\kappa L}} = \frac{1 + \rho\varepsilon^2}{1 + \frac{\varepsilon^2}{2\kappa}} = 1 + \left( \rho - \frac{1}{2\kappa} \right) \varepsilon^2 + \mathcal{O}(\varepsilon^4), \quad (4.122)$$

$$m^2 = \left( 2\rho - \frac{1}{\kappa} \right) + \mathcal{O}(\varepsilon^2). \quad (4.123)$$

We note that now we have that  $m = \mathcal{O}(1)$ , instead of the order  $\mathcal{O}(1/\varepsilon)$  that we had before. The wave equation becomes

$$Y_{tt}(x, t) = Y_{xx}(x, t) + \varepsilon^2 \frac{\Gamma}{2} Y_{xx}(x, t) \left( \int_0^L Y_x^2(\xi, t) d\xi - \varepsilon^2 \sqrt{2\rho - \frac{1}{\kappa}} \int_0^L Y_x(\xi, t) d\xi + \left(2\rho - \frac{1}{\kappa}\right) \varepsilon^2 \right) \quad (4.124)$$

$$= Y_{xx}(x, t) + \frac{\varepsilon^2}{2} Y_{xx}(x, t) \int_0^L Y_x^2(\xi, t) d\xi + \mathcal{O}(\varepsilon^4). \quad (4.125)$$

So we can see that we obtain the same nonlinear string equation that we had before. For the forces on the boundary, we obtain

$$F_T = -m\varepsilon^2 + Y_x(0, t) - \frac{1}{2}\varepsilon^2 Y_x^3(0, t) + \mathcal{O}(\varepsilon^4), \quad (4.126)$$

$$F_s = -m\varepsilon^2 + \kappa \left(4\rho - \frac{3}{\kappa}\right) \varepsilon^2 Y(0, t) + 3\kappa \sqrt{2\rho - \frac{1}{\kappa}} \varepsilon^2 Y^2(0, t) + \kappa \varepsilon^2 Y^3(0, t) + \mathcal{O}(\varepsilon^4), \quad (4.127)$$

$$F_d = 2\alpha Y_t(0, t) \left[ \left(2\rho - \frac{1}{\kappa}\right) \varepsilon^2 + 2\sqrt{2\rho - \frac{1}{\kappa}} \varepsilon^2 Y(0, t) + 2\varepsilon^2 Y^2(0, t) + \mathcal{O}(\varepsilon^4) \right]. \quad (4.128)$$

We can see that all the extra terms due to the new expansion are pushed to the  $\mathcal{O}(\varepsilon^2)$  order or higher orders. This simplifies our equations, and it makes sure that we can use the previous method to solve this system. Furthermore, we can see that the constant terms in  $F_T$  and  $F_s$  cancel out.

However, due to the order assumptions, we also see that we obtain new bounds on the parameters. The first is that  $2\rho - 1/\kappa > 0$ , and if we do not satisfy the bound, we see that we would have  $\ell_{eq} < 1$ . This means that in the current ordering, the tension force is stronger than the spring force, and so the springs cannot push the string out of the zero position. The second bound is  $4\rho - 3/\kappa > 0$ , since we want the linear term of the spring force to be a restoring force. We can see that if we satisfy the second constraint, we will also satisfy the first constraint.

So our final system of  $Y(x, t)$  is given by

$$Y_{tt}(x, t) = Y_{xx}(x, t) + \frac{\varepsilon^2}{2} Y_{xx}(x, t) \int_0^L Y_x^2(\xi, t) d\xi, \quad 0 < x < L, t > 0, \quad (4.129a)$$

$$Y_x - \frac{1}{2}\varepsilon^2 Y_x^3 = \beta Y_t + \varepsilon^2 \left[ (4\rho\kappa - 3)Y + 3\kappa \sqrt{2\rho - \frac{1}{\kappa}} Y^2 + \kappa Y^3 + 2\alpha Y_t \left( 2\rho - \frac{1}{\kappa} + 2\sqrt{2\rho - \frac{1}{\kappa}} Y + 2Y^2 \right) \right], \quad x = 0, t > 0, \quad (4.129b)$$

$$Y(L, t) = 0, \quad t > 0. \quad (4.129c)$$

We do not specify the initial conditions here since those are determined when matching the stable region to the unstable region.

We will follow the same steps as before. So we introduce the two time scales  $t_0 = t$  and  $t_1 = \varepsilon^2 t$  and expand  $Y(x, t_0, t_1) = Y_0(x, t_0, t_1) + \varepsilon^2 Y_1(x, t_0, t_1) + \mathcal{O}(\varepsilon^4)$ . Then we obtain the following first-order system

$$\mathcal{O}(1) : Y_{0,t_0 t_0} = Y_{0,xx}, \quad 0 < x < L, t_0, t_1 > 0, \quad (4.130)$$

$$Y_{0,x} = \beta Y_{0,t_0}, \quad x = 0, t_0, t_1 > 0, \quad (4.131)$$

$$Y_0(L, t_0, t_1) = 0, \quad t_0, t_1 > 0. \quad (4.132)$$

This is the same system as we solved above. Thus, we know that the solution is given as

$$Y_0(x, t_0, t_1) = \sum_n \hat{\varphi}_n(x) D_n(t_1) e^{s_n t_0}, \quad (4.133)$$

where  $D_n(t_1)$  has to be determined by the second time scale and  $s_n$  are the same eigenvalues as in the unstable region. For the second time scale we obtain after homogenization of the boundary condition the

same system as Equation (4.59), again with  $\lambda = 0$ ,  $\zeta$  replaced by  $\hat{\zeta}$  and  $\hat{h}(t_0, t_1)$  replaced by

$$H_{compr}(t_0, t_1) = \left[ \beta Y_{0,t_1} + \frac{1}{2} \varepsilon^2 Y_{0,x}^3 + (4\rho\kappa - 3)Y_0 + 3\kappa \sqrt{2\rho - \frac{1}{\kappa}} Y_0^2 + \kappa Y_0^3 \right. \\ \left. + 2\alpha Y_{0,t_0} \left( 2\rho - \frac{1}{\kappa} + 2\sqrt{2\rho - \frac{1}{\kappa}} Y_0 + 2Y_0^2 \right) \right]_{(0,t_0,t_1)}. \quad (4.134)$$

We now also have quadratic terms, which can create resonances. However, since the real part of the poles is still constant, we have that the quadratic terms do not result in resonances. By letting the linear terms cancel, we obtain that

$$\int_0^L \left[ 2s_n \varphi_n(x) \hat{\varphi}_n(x) + \left( \frac{x}{L} - 1 \right) \varphi_n(x) \frac{s_n^2}{s_n + \hat{\zeta}} \hat{\varphi}_n(0) \right] dx \cdot D'_n(t_1) = \\ - \int_0^L \left( \frac{x}{L} - 1 \right) \varphi_n(x) dx \hat{\varphi}_n(0) \frac{s_n^2}{\beta(s_n + \hat{\zeta})} \left( 4\rho\kappa - 3 + 2s_n\alpha \left( 2\rho - \frac{1}{\kappa} \right) \right) D_n(t_1). \quad (4.135)$$

Thus, it follows that

$$D_n(t_1) = E_n e^{-Z_n(4\rho\kappa - 3 + 2s_n\alpha(2\rho - \frac{1}{\kappa}))t_1} = E_n e^{-Z_n\Lambda_n t_1}, \quad (4.136)$$

where we have defined  $\Lambda_n = 4\rho\kappa - 3 + 2s_n\alpha(2\rho - \frac{1}{\kappa})$ . The constant  $E_n$  has to be determined by matching the two solutions together. Due to the assumptions on  $\kappa$  and  $\rho$ , we can see that in  $\Lambda_n$  we have that almost all the terms are positive, except for  $\Re(s_n)$ . However, since  $\Re(s_n) = \mathcal{O}(\varepsilon^2)$  we expect that  $\Re(\Lambda_n) > 0$ . We note that for  $\beta = \mathcal{O}(1/\varepsilon^{2/3})$  and  $n = 0$ , we obtain  $Z'_0\Lambda_0$  in the exponent.

To match the two solutions, we will first need a series representation of  $u_{eq}(x)$ . This can be found by using the first-order solution Equation (4.96) with  $u_{eq}(x)$  as its initial conditions and without the time dependency. So we have that  $f(x) = u_{eq}(x)$  and  $g(x) = 0$ . Thus the series representation becomes

$$u_{eq}(x) = \sum_n \hat{\varphi}_n(x) \left( - \int_0^L s_n u_{eq}(\xi) \varphi_n(\xi) d\xi - 2 \frac{\beta}{\beta + 1} u_{eq}(0) \right) = \frac{m}{L} (1 - \gamma_0) \sum_n \frac{\hat{\varphi}_n(x)}{s_n}. \quad (4.137)$$

We will match on the value at the boundary  $x = 0$ , since the instability originates from the boundary condition. We have to choose a threshold value  $u_0 = u^*$ , which is reached at time  $t_0^* = t^*$  and  $t_1^* = \varepsilon^2 t^*$ . Any value between the two equilibrium positions can be chosen, so for this we will use  $u^* = \frac{1}{2} u_{eq}(0) = \frac{1}{2} m$ . Now using that  $Y_0(x, t_0^*, t_1^*) = u_0(x, t_0^*, t_1^*) - u_{eq}(x)$ , we can see that

$$\sum_n \hat{\varphi}_n(0) E_n e^{-Z_n \Lambda_n t_1^*} e^{s_n t_0^*} = \sum_n \hat{\varphi}_n(0) C_n e^{Z_n \hat{\lambda} t_1^*} e^{s_n t_0^*} - \frac{m}{L} (1 - \gamma_0) \sum_n \frac{\hat{\varphi}_n(0)}{s_n}. \quad (4.138)$$

It can be noted from above that it does not matter on which  $x$  position we match, since each sum has the  $\hat{\varphi}_n(x)$  term. Consequently, we have that

$$E_n = \left[ C_n e^{Z_n \hat{\lambda} t_1^*} - \frac{m(1 - \gamma_0)}{s_n L} e^{-s_n t_0^*} \right] e^{Z_n \Lambda_n t_1^*}. \quad (4.139)$$

For when we need to switch from the stable region back into the unstable region, we can use the same process as above.

Above, we have done the solution for the upper stable equilibrium point; however, there is also a lower equilibrium point. For this region, we introduce  $\mathcal{Y}(x, t) = u(x, t) + u_{eq}(x)$  and then we can follow the same steps. The only change is that in Equations (4.119)–(4.121) the terms with even powers of  $Y$  have their sign flipped. However, since the constant terms cancel and the quadratic terms do not result in resonances, we have that the constants,  $E_n$  and  $\Lambda_n$ , do not change.

In Figure 14, the reflection of the wave for different times is shown. It has the same parameters as the plots in Figure 13b. The plots start from  $t = 6\pi$ , since the matching time is  $t^* = 7.02\pi$ . Additionally, the equilibrium position,  $u_{eq}(x)$ , is also shown in the plots. From the plots which straddle the matching time,  $t = 7\pi$  and  $t = 8\pi$ , we can see that the solution stays continuous. However, after the matching, we can see a small angle in the solution, which travels downward. This is due to the solution not being continuous in  $t_1$ , by the change in the exponent.

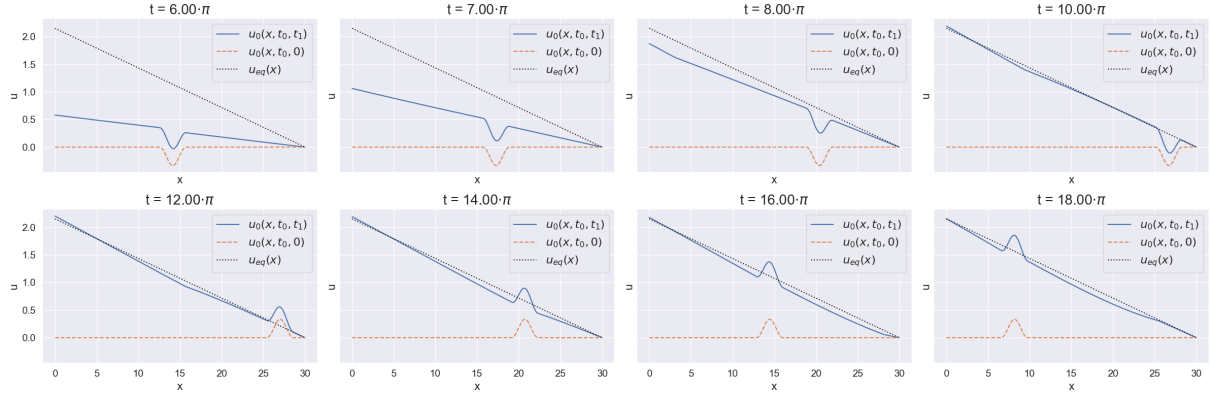


**Figure 14:** Plots of the multiple time scale solution for  $\beta = 1.5$ ,  $\kappa = 2$ ,  $\rho = 2.5$  and  $\alpha = 1$ . The matching time corresponding to these parameters is  $t^* = 13.28$ .

### 4.2.3 Energy analysis

We defined the energy of the system in Equation (3.29), however, that was before we introduced the second time scale. By splitting the time derivative into its  $t_0$  and  $t_1$  parts, we obtain that

$$E(t) = \frac{\varepsilon^2}{2} \int_0^L [u_{t_0}^2 + u_x^2] dx + \kappa(\sqrt{1 + \varepsilon^2 u^2(0, t)} - \ell_0)^2 + \varepsilon^4 \int_0^L u_{t_0} u_{t_1} dx + \frac{\varepsilon^6}{2} \int_0^L u_{t_1}^2 dx. \quad (4.140)$$

We can also apply our ordering assumption to the energy contribution of the boundary condition, so we obtain

$$\kappa(\sqrt{1 + \varepsilon^2 u^2(0, t)} - \ell_0)^2 = \kappa \varepsilon^4 \left( \frac{1}{2} u^2(0, t) - \rho + \mathcal{O}(\varepsilon^2) \right)^2 = \kappa \varepsilon^4 \left( \frac{1}{2} u^2(0, t) - \rho \right)^2 + \mathcal{O}(\varepsilon^6). \quad (4.141)$$

We can see that the linear energy term should give the largest contribution to the energy of the system. In practice, we use the full expression of the boundary energy term, since it is not much more computationally expensive.

In Figure 15, the energy of the system for different parameter sets is plotted. For each parameter set the matching time  $t^*$  is also given in the legend. We have split the energy into its four different parts to highlight the contribution of each term. The first part,  $E_{lin}$ , is the linear energy integral and  $E_{bnd}$  is  $E_{lin}$  plus the energy of the boundary. For  $E_{bnd}$ , we have subtracted the initial energy of the boundary system,  $\kappa \ell_0^2$ , to shift the starting energy to the same position.  $E_{mix}$  is  $E_{bnd}$  plus the integral of the product of the two time derivatives. Finally,  $E_{full}$  is the full equation Equation (4.140).

We first consider the case where we have changed the coefficient of the oblique damper,  $\alpha$ . In Figure 15a, we can see that before the matching time, the values of the energies are the same. This is as expected since the oblique damper is not present in the first order. Furthermore, we can see that the profile of the energy plot looks similar to the plots in Figure 7, because the first order of both solutions is the same. In the middle of the collision, we can see that  $E_{bnd}$  and the other corrections are slightly different from the linear energy. After the matching time, we can see that the energy increases and the increase is more noticeable for higher values of  $\alpha$ . To understand this, we have to consider the product  $-Z_n \Lambda_n$ , we have that

$$-Z_n \Lambda_n = \frac{1}{\beta^2 - 1} \left[ \frac{1}{s_n L} (4\rho\kappa - 3) + 2\alpha\varepsilon^2 \left( 2\rho - \frac{1}{\kappa} \right) \right]. \quad (4.142)$$

We can see that the first term is negative and thus has a stable contribution. But as  $n$  becomes larger, that term will become smaller until the positive term dominates. Thus, for larger  $n$ , the exponent will be positive and thus the solution will grow, and as we see, the growth is more pronounced for larger  $\alpha$ . However, this increase in energy violates the energy conservation that has been shown. It is unclear what causes this behaviour, but it is likely due to the multiple time scale method not correctly capturing the dynamics as seen before.

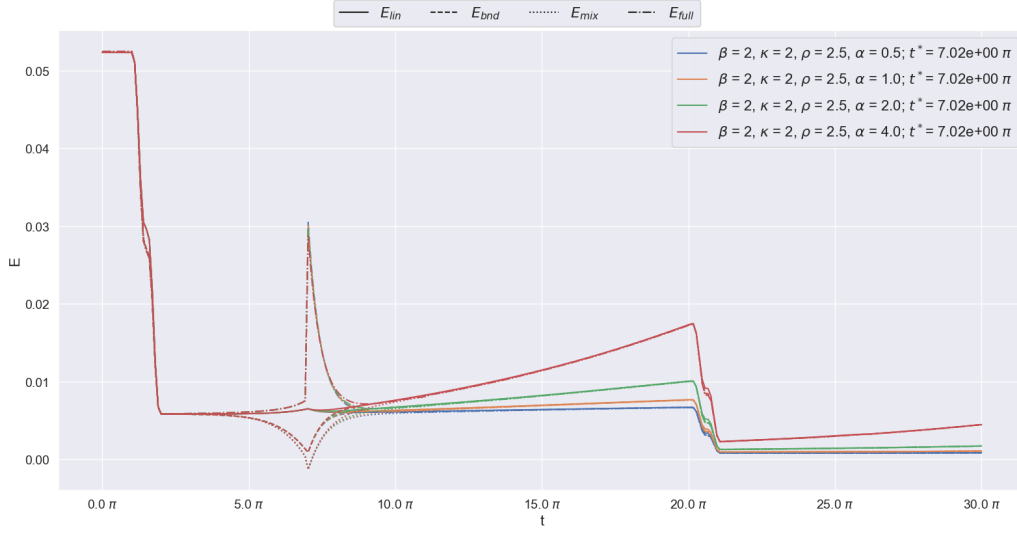
Finally, we see that in general, the other energies,  $E_{bnd}$ ,  $E_{mix}$  and  $E_{full}$ , are almost the same as  $E_{lin}$ . However that around the matching time, the other energies differ significantly. This is likely because in the transition region, the error increases. We have that the addition of the boundary energy has a

significant contribution to the energy, it is slightly more than the expected order of  $\varepsilon^2$ . Furthermore, we can see that the mixed term has only a small contribution. However, we see that the square term,  $u_{t_1}^2$ , has about the same contribution as the boundary term, while it should be an order of  $\varepsilon^2$  smaller. Additionally, in the  $E_{full}$  term, there is a discontinuity in the energy. This is because  $u_{t_1}$  is not continuous due to the difference in the factor in the exponent.

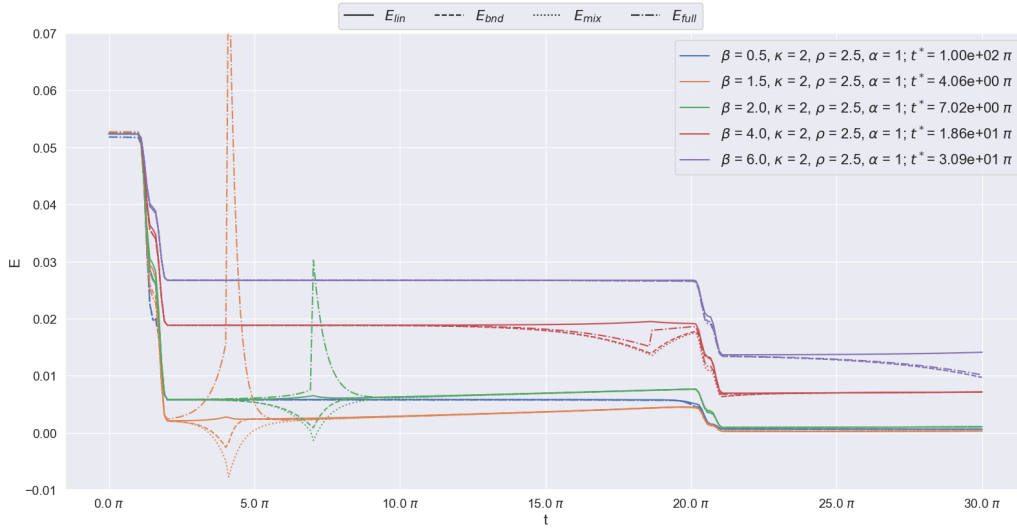
Now let us consider the case where we vary the parameter  $\beta$ , which is shown in [Figure 15b](#). First, we have shown only one case where  $\beta < 1$ , since the solution stays stable, the energy is comparable to the first order energy. The matching time is given as  $t = 100\pi$ , however, this is because it is never reached and thus the maximum value for the calculation is shown

Now, for  $\beta > 1$ , we can see that as  $\beta$  becomes larger, the matching time also increases. Furthermore, we note that as  $\beta$  becomes closer to 1, the peaks of  $E_{full}$  become larger. This is because the fraction  $Z_n$  grows as  $\beta$  goes towards 1 and thus the contribution of  $u_{t_1}$  becomes larger. Lastly, we can see that for low values of  $\beta$ , there is an increase in energy, which becomes less for larger values of  $\beta$ . This is the same as what we saw for higher values of  $\alpha$ . However, for the smaller values of  $\beta$ , this more noticeable effect is due to the factor  $1/(\beta^2 - 1)$ .

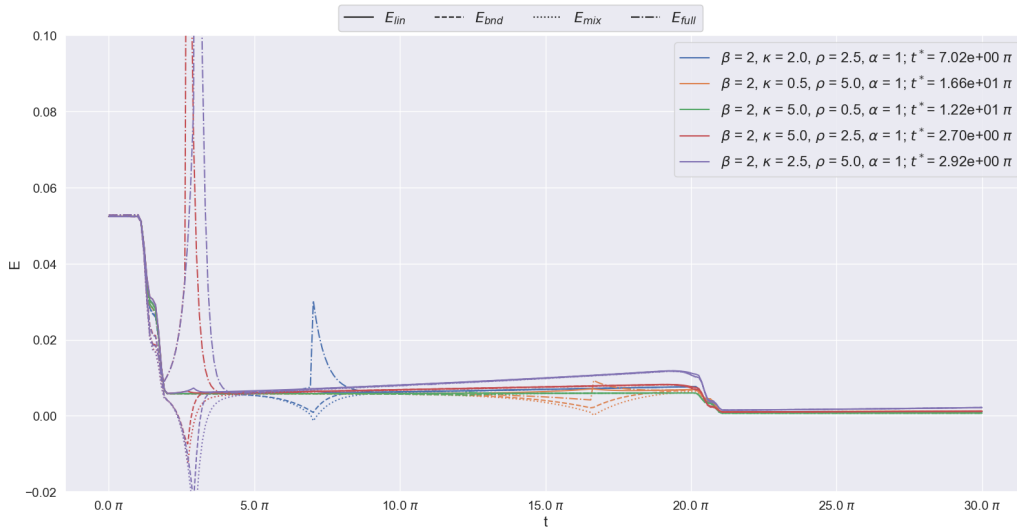
Finally, we turn to the different parameters for the springs in [Figure 15c](#). Next to the default parameter set, we have shown two pairs such that we have two different values of  $\hat{\lambda} = 2\kappa\rho$  with the two possible permutations of  $\kappa$  and  $\rho$ . We can see that as  $\hat{\lambda}$  increases that the matching time decreases, since the nonlinear system is stronger to push the string out of its unstable position. Furthermore, we can see that for bigger values of  $\rho$ , we have a larger error when matching. This is because the equilibrium position is further away, and so the unstable and stable regions become larger, which causes the matching point to also be further away. This is most noticeable for  $\kappa = 5$  and  $\rho = 0.5$ , since it has almost no difference between the energies. Lastly, we again see an increase in energy, which is stronger for higher values of  $\rho$ .



(a) Energies of the system for different values of  $\alpha$ .



(b) Energies of the system for different values of  $\beta$ .



(c) Energies of the system for different values of  $\kappa$  and  $\rho$ .

**Figure 15:** Plots of the energy of the system and its corrections for different parameter groups.

## 5 Conclusion

This report investigated the behaviour of a nonlinear string system with a quasi-zero stiffness (QZS) boundary condition, focusing on the system's reflection and absorption properties. First, a regular perturbation analysis was performed, which was solved using the d'Alembert solution. Due to the appearance of linear growth in the second order, the method of multiple time scales was applied next. The system originating from this was solved using the Laplace transform.

The model was split into cases where the oblique springs were extended or compressed. When the springs were extended, it was seen that the multiple time scale solution did not differ from the first-order solution. For the case with the compressed springs, the system was unstable if the coefficient of the vertical damper, denoted by  $\beta$ , was larger than one. However, if  $\beta$  was smaller than one, the model produced a stable system. This outcome was unexpected as it contradicts the physical intuition for the system's behaviour. The discrepancy arises due to the singular nature of the system's poles and the influence of the multiple time scale method used. Furthermore, the addition of oblique dampers produced an unexpected instability in the system. Instead of dissipating energy as intended, the dampers led to an increase in the system's energy even when the solution was at what should have been a stable equilibrium. This counterintuitive behaviour suggests that the multiple time scale method may again be responsible, as its approximations may fail to capture subtle interactions or nonlinear effects introduced by the dampers. Lastly, it emerged that when matching the unstable and stable regions, higher compression of the springs and higher spring constants resulted in higher errors in the boundary region. This was due to the stronger nonlinear effects present in the system.

To address the unexpected results in this study, namely the stability for  $\beta < 1$  and the destabilising effect of oblique dampers, it is recommended to consider alternative asymptotic expansions or techniques. They should be explored to determine whether they offer a more accurate representation of the system's dynamics. Furthermore, it is recommended to improve the analytical model by incorporating second-order terms for the multiple time scale expansion, which would allow more of the nonlinear dynamics to be studied. Finally, applying harmonic forcing to the system could provide deeper insights into its damping characteristics and practical applicability. By introducing a periodic input, one can analyse the system's frequency response and identify resonant frequencies, amplitude amplification effects, and phase relationships.

## References

- [1] C. Geurts, T. Vrouwenvelder, P. van Staalduinen, and J. Reusink, “Numerical Modelling of Rain-Wind-Induced Vibration: Erasmus Bridge, Rotterdam”, *Structural Engineering International*, vol. 8, no. 2, pp. 129–135, May 1998, Publisher: Taylor & Francis \_eprint: <https://doi.org/10.2749/101686698780489351>, ISSN: 1016-8664. DOI: [10.2749/101686698780489351](https://doi.org/10.2749/101686698780489351). [Online]. Available: <https://doi.org/10.2749/101686698780489351> (visited on 10/22/2024).
- [2] *Forced Damped Oscillator*, Jul. 2022.
- [3] R. A. Ibrahim, “Recent advances in nonlinear passive vibration isolators”, *Journal of Sound and Vibration*, vol. 314, no. 3, pp. 371–452, Jul. 2008, ISSN: 0022-460X. DOI: [10.1016/j.jsv.2008.01.014](https://doi.org/10.1016/j.jsv.2008.01.014). [Online]. Available: <https://www.sciencedirect.com/science/article/pii/S0022460X08000436> (visited on 10/23/2024).
- [4] Z. Ma, R. Zhou, and Q. Yang, “Recent Advances in Quasi-Zero Stiffness Vibration Isolation Systems: An Overview and Future Possibilities”, en, *Machines*, vol. 10, no. 9, p. 813, Sep. 2022, Number: 9 Publisher: Multidisciplinary Digital Publishing Institute, ISSN: 2075-1702. DOI: [10.3390/machines10090813](https://doi.org/10.3390/machines10090813). [Online]. Available: <https://www.mdpi.com/2075-1702/10/9/813> (visited on 09/11/2024).
- [5] W. G. Molyneux, “Supports for vibration isolation”, en, *Her Majesty’s Stationery Office: London, UK*, 1957, Accepted: 2014-10-20T11:01:17Z. [Online]. Available: <https://reports.aerade.cranfield.ac.uk/handle/1826.2/335> (visited on 10/02/2024).
- [6] A. Carrella, M. J. Brennan, and T. P. Waters, “Static analysis of a passive vibration isolator with quasi-zero-stiffness characteristic”, *Journal of Sound and Vibration*, vol. 301, no. 3, pp. 678–689, Apr. 2007, ISSN: 0022-460X. DOI: [10.1016/j.jsv.2006.10.011](https://doi.org/10.1016/j.jsv.2006.10.011). [Online]. Available: <https://www.sciencedirect.com/science/article/pii/S0022460X06007954> (visited on 09/11/2024).
- [7] A. Carrella, M. J. Brennan, T. P. Waters, and V. Lopes, “Force and displacement transmissibility of a nonlinear isolator with high-static-low-dynamic-stiffness”, *International Journal of Mechanical Sciences*, vol. 55, no. 1, pp. 22–29, Feb. 2012, ISSN: 0020-7403. DOI: [10.1016/j.ijmecsci.2011.11.012](https://doi.org/10.1016/j.ijmecsci.2011.11.012). [Online]. Available: <https://www.sciencedirect.com/science/article/pii/S0020740311002475> (visited on 09/11/2024).
- [8] B. Yan, N. Yu, H. Ma, and C. Wu, “A theory for bistable vibration isolators”, *Mechanical Systems and Signal Processing*, vol. 167, p. 108 507, Mar. 2022, ISSN: 0888-3270. DOI: [10.1016/j.ymsp.2021.108507](https://doi.org/10.1016/j.ymsp.2021.108507). [Online]. Available: <https://www.sciencedirect.com/science/article/pii/S0888327021008499> (visited on 09/09/2024).
- [9] M. J. Brennan, I. Kovacic, A. Carrella, and T. P. Waters, “On the jump-up and jump-down frequencies of the Duffing oscillator”, *Journal of Sound and Vibration*, vol. 318, no. 4, pp. 1250–1261, Dec. 2008, ISSN: 0022-460X. DOI: [10.1016/j.jsv.2008.04.032](https://doi.org/10.1016/j.jsv.2008.04.032). [Online]. Available: <https://www.sciencedirect.com/science/article/pii/S0022460X08003805> (visited on 09/11/2024).
- [10] Y. Qiu, Y. Zhu, Z. Luo, Y. Gao, and Y. Li, “The analysis and design of nonlinear vibration isolators under both displacement and force excitations”, en, *Archive of Applied Mechanics*, vol. 91, no. 5, pp. 2159–2178, May 2021, ISSN: 1432-0681. DOI: [10.1007/s00419-020-01875-0](https://doi.org/10.1007/s00419-020-01875-0). [Online]. Available: <https://doi.org/10.1007/s00419-020-01875-0> (visited on 09/11/2024).
- [11] R. Xie, K. Xu, H. Kang, and L. Zhao, “Multimodal vortex-induced vibration mitigation and design approach of bistable nonlinear energy sink inerter on bridge structure”, *Journal of Infrastructure Intelligence and Resilience*, p. 100 123, Sep. 2024, ISSN: 2772-9915. DOI: [10.1016/j.iintel.2024.100123](https://doi.org/10.1016/j.iintel.2024.100123). [Online]. Available: <https://www.sciencedirect.com/science/article/pii/S2772991524000422> (visited on 09/12/2024).
- [12] R. Narasimha, “Non-Linear vibration of an elastic string”, *Journal of Sound and Vibration*, vol. 8, no. 1, pp. 134–146, Jul. 1968, ISSN: 0022-460X. DOI: [10.1016/0022-460X\(68\)90200-9](https://doi.org/10.1016/0022-460X(68)90200-9). [Online]. Available: <https://www.sciencedirect.com/science/article/pii/0022460X68902009> (visited on 09/19/2024).
- [13] B. Tang and M. J. Brennan, “A comparison of two nonlinear damping mechanisms in a vibration isolator”, *Journal of Sound and Vibration*, vol. 332, no. 3, pp. 510–520, Feb. 2013, ISSN: 0022-460X. DOI: [10.1016/j.jsv.2012.09.010](https://doi.org/10.1016/j.jsv.2012.09.010). [Online]. Available: <https://www.sciencedirect.com/science/article/pii/S0022460X12006992> (visited on 09/18/2024).

- [14] T. Akkaya and W. T. van Horssen, “Reflection and damping properties for semi-infinite string equations with non-classical boundary conditions”, *Journal of Sound and Vibration*, vol. 336, pp. 179–190, Feb. 2015, ISSN: 0022-460X. DOI: [10.1016/j.jsv.2014.10.014](https://doi.org/10.1016/j.jsv.2014.10.014). [Online]. Available: <https://www.sciencedirect.com/science/article/pii/S0022460X14008293> (visited on 09/10/2024).
- [15] R. Haberman, *Applied Partial Differential Equations: With Fourier Series and Boundary Value Problems*, en. Pearson, 2013, Google-Books-ID: hGNwLgEACAAJ, ISBN: 978-0-321-79705-6.
- [16] P. Virtanen, R. Gommers, T. E. Oliphant, *et al.*, “SciPy 1.0: Fundamental algorithms for scientific computing in Python”, en, *Nature Methods*, vol. 17, no. 3, pp. 261–272, Mar. 2020, Publisher: Nature Publishing Group, ISSN: 1548-7105. DOI: [10.1038/s41592-019-0686-2](https://doi.org/10.1038/s41592-019-0686-2). [Online]. Available: <https://www.nature.com/articles/s41592-019-0686-2> (visited on 02/14/2025).
- [17] R. H. Byrd, P. Lu, J. Nocedal, and C. Zhu, “A Limited Memory Algorithm for Bound Constrained Optimization”, *SIAM Journal on Scientific Computing*, vol. 16, no. 5, pp. 1190–1208, Sep. 1995, Publisher: Society for Industrial and Applied Mathematics, ISSN: 1064-8275. DOI: [10.1137/0916069](https://doi.org/10.1137/0916069). [Online]. Available: <https://epubs.siam.org/doi/abs/10.1137/0916069> (visited on 02/14/2025).
- [18] C. Zhu, R. H. Byrd, P. Lu, and J. Nocedal, “Algorithm 778: L-BFGS-B: Fortran subroutines for large-scale bound-constrained optimization”, *ACM Trans. Math. Softw.*, vol. 23, no. 4, pp. 550–560, Dec. 1997, ISSN: 0098-3500. DOI: [10.1145/279232.279236](https://doi.org/10.1145/279232.279236). [Online]. Available: <https://dl.acm.org/doi/10.1145/279232.279236> (visited on 02/14/2025).
- [19] W. D. Vernon, *The Laplace Transform*, eng. Princeton University Press, Princeton, 1946. [Online]. Available: <http://archive.org/details/dli.ernet.206074> (visited on 05/16/2025).

## A Appendix: Code

The code used for this project can be found on:

<https://github.com/jvdv1912/Vibrations-of-a-nonlinear-string>.